the plant journal

SEB SOCIETY FOR EXPERIMENTAL BIOLOGY

The Plant Journal (2021) **106,** 733–752 doi: 10.1111/tpj.15195

Comparative transcriptome profiling identifies maize line specificity of fungal effectors in the maize–*Ustilago maydis* interaction

Selma Schurack[1,2], Jasper R.L. Depotter[1], Deepak Gupta[3,4], Marco Thines[3,4] and Gunther Doehlemann[1,*]

[1]*CEPLAS, Institute for Plant Sciences, University of Cologne, Cologne, Germany,*

[2]*IMPRS, Max Planck Institute for Plant Breeding Research, Cologne, Germany,*

[3]*Senckenberg Biodiversity and Climate Research Centre (BiK-F), Frankfurt a. M, Germany, and*

[4]*Institute of Ecology, Evolution and Diversity, Goethe University, Frankfurt, Frankfurt a. M, Germany*

Received 18 November 2020; revised 3 February 2021; accepted 8 February 2021; published online 12 February 2021.
*For correspondence (e-mail g.doehlemann@uni-koeln.de).

SUMMARY

The biotrophic pathogen *Ustilago maydis* causes smut disease on maize (*Zea mays*) and induces the formation of tumours on all aerial parts of the plant. Unlike in other biotrophic interactions, no gene-for-gene interactions have been identified in the maize–*U. maydis* pathosystem. Thus, maize resistance to *U. maydis* is considered a polygenic, quantitative trait. Here, we study the molecular mechanisms of quantitative disease resistance (QDR) in maize, and how *U. maydis* interferes with its components. Based on quantitative scoring of disease symptoms in 26 maize lines, we performed an RNA sequencing (RNA-Seq) analysis of six *U. maydis*-infected maize lines of highly distinct resistance levels. The different maize lines showed specific responses of diverse cellular processes to *U. maydis* infection. For *U. maydis*, our analysis identified 406 genes being differentially expressed between maize lines, of which 102 encode predicted effector proteins. Based on this analysis, we generated *U. maydis* CRISPR/Cas9 knock-out mutants for selected candidate effector sets. After infections of different maize lines with the fungal mutants, RNA-Seq analysis identified effectors with quantitative, maize line-specific virulence functions, and revealed auxin-related processes as a possible target for one of them. Thus, we show that both transcriptional activity and virulence function of fungal effector genes are modified according to the infected maize line, providing insights into the molecular mechanisms underlying QDR in the maize–*U. maydis* interaction.

Keywords: *Ustilago maydis*, *Zea mays*, transcriptome analysis, effectors, quantitative disease resistance, CRISPR-Cas9.

INTRODUCTION

In natural environments, plants are constantly exposed to a variety of potentially pathogenic microbes. To protect themselves, they have evolved multiple layers of immune responses and in turn, microbes have developed so-called effectors to cope with or suppress these immune responses. Current studies in molecular plant pathology have mainly focused on understanding the molecular mechanisms of qualitative resistance, which is determined by large-effect resistance (R) genes leading to almost complete resistance or susceptibility. This is often conferred by nucleotide-binding leucine-rich repeat (NLR) receptors (Cui *et al.*, 2015; Dangl and Jones, 2001; McHale *et al.*, 2006). In contrast, quantitative disease resistance (QDR) still remains poorly understood (Corwin and Kliebenstein, 2017; Poland *et al.*, 2009; Roux *et al.*, 2014), even though it determines the outcome of the majority of plant–pathogen interactions in crops and natural populations (Bartoli and Roux, 2017). In QDR, many genes with small to moderate effects lead to a continuous distribution of susceptible to resistant phenotypes (Niks *et al.*, 2015; Poland *et al.*, 2009; Roux *et al.*, 2014; St. Clair, 2010).

Many QDR loci have been mapped in the past, but the underlying complex genetic architecture has limited the molecular characterisation of mechanisms involved (Corwin and Kliebenstein, 2017). Still, several QDR genes with various functions have been cloned recently. In several cases, kinases have been shown to play important roles in QDR. Two maize (*Zea mays*) wall-associated kinases, ZmWAK-RLK1 and ZmWAK, confer QDR to northern corn leaf blight and head smut, respectively (Hurni *et al.*, 2015; Zuo *et al.*, 2015). Other QDR genes encode putative

transporters, and the ATP-binding cassette (ABC) transporter encoded by *Lr34* confers resistance to diverse fungal pathogens in wheat (*Triticum aestivum*) (Krattinger *et al.*, 2009). A caffeoyl-CoA O-methyltransferase connected to lignin production was shown to confer QDR to various necrotrophic maize pathogens (Yang *et al.*, 2017). Other genes identified in QDR correspond to previously unidentified defence genes, such as the soybean (*Glycine max*) wound-inducible domain protein WI12, the soybean serine hydroxymethyltransferase RHG4 and the rice (*Oryza sativa*) proline-containing protein Pi21 (Cook *et al.*, 2012; Fukuoka *et al.*, 2009). In rare cases, NLR genes can also underlie QDR (Barbacci *et al.*, 2020; Poland *et al.*, 2009), which led to the hypothesis that allelic variants, i.e. weak alleles, of R genes can cause incomplete resistance. Thus, compared to qualitative resistance, the molecular functions underlying QDR seem to be highly diverse. Additionally, studies of QDR by RNA sequencing (RNA-Seq) approaches have indicated highly interconnected and multifaceted defence responses, which were mostly distinct from functions previously identified for plant immunity (Delplace *et al.*, 2020; Kebede *et al.*, 2018; Pan *et al.*, 2018).

The biotrophic fungus *Ustilago maydis* causes smut disease in maize. Characteristic disease symptoms are tumours that can be formed on all aboveground organs of maize plants in less than 2 weeks after infection (Basse and Steinberg, 2004; Kämper *et al.*, 2006). *Ustilago maydis* has advanced to a model for biotrophic plant pathogens due to its rapid symptom development, very compact genome, easy *in vitro* cultivation and accessibility to genetic manipulation (Brefort *et al.*, 2009; Dean *et al.*, 2012; Kämper, 2004; Schuster *et al.*, 2016; Zuo *et al.*, 2020; Zuo *et al.*, 2019). The infection cycle of *U. maydis* is initiated by recognition and fusion of sporidia with compatible mating types, leading to a morphological switch from yeast-like haploid cells to diploid filaments (Bölker *et al.*, 1992; Spellig *et al.*, 1994). The generation of the solopathogenic strain SG200, derived from a field isolate collected in Minnesota, USA, and genetically engineered to be able to form infectious filaments without prior mating, has greatly facilitated the investigation of *U. maydis* pathogenic development (Kämper *et al.*, 2006). Dutheil *et al.* (2016) predicted 553 candidate secreted effector proteins encoded in the genome of *U. maydis*. This prediction includes proteins which contain a signal peptide for secretion, as well as a predicted extracellular location, and most of them lack any known functional or structural domains (Dutheil *et al.*, 2016). Many effectors reside in clusters in the genome, are expressed specifically during biotrophic development compared to axenic culture and contribute to virulence (Kämper *et al.*, 2006; Müller *et al.*, 2008; Schilling *et al.*, 2014; Schirawski *et al.*, 2010; Skibbe *et al.*, 2010). However, so far only a few individual effectors with large effects on virulence have been functionally characterised (Djamei *et al.*, 2011; Doehlemann *et al.*, 2009; Ma *et al.*, 2018; Ökmen *et al.*, 2018; Redkar *et al.*, 2015; Tanaka *et al.*, 2014, Sharma *et al.*, 2019). Despite *U. maydis* being the predominant model organism of biotrophic plant pathogens, resistance to *U. maydis* has been rarely described (Baumgarten *et al.*, 2007; Lübberstedt *et al.*, 1998). Unlike in other biotrophic interactions, no gene-for-gene interactions have been identified in the *U. maydis*–maize pathosystem. Crosses of *U. maydis*-resistant and -susceptible maize lines have previously indicated that *U. maydis* resistance is a polygenic, quantitative trait (Hoover, 1932; Immer, 1927). Several QDR loci that contribute to *U. maydis* infection frequency and severity have been identified, and some studies have suggested that specific loci may contribute to *U. maydis* resistance in an organ-specific manner (Baumgarten *et al.*, 2007; Lübberstedt *et al.*, 1998). Interestingly, several QDR loci conferring resistance to *U. maydis* contain genes with a known role in defence against pathogens, such as NLRs, a pathogenesis-related protein, a chitinase, a basal antifungal protein and a wound-inducible protein (Baumgarten *et al.*, 2007; Brefort *et al.*, 2009). For one *U. maydis* effector, ApB73, a maize line-specific virulence function has been observed (Stirnberg and Djamei, 2016). This suggests that the fungus' effectors might target certain host genes contributing to QDR. However, the molecular basis of QDR in maize and how *U. maydis* interferes with its components is still mostly unknown.

Extensive transcriptome analyses have revealed organ-, cell type- and stage-specific expression patterns of the *U. maydis* effector gene repertoire (Lanver *et al.*, 2018; Matei *et al.*, 2018; Skibbe *et al.*, 2010). Despite these efforts, how gene expression is influenced by host lines of quantitatively different resistance levels remains to be elucidated. Such knowledge would help to draw a more comprehensive picture of *U. maydis* virulence.

In this study, we analysed the transcriptome of *U. maydis* infecting six maize lines of quantitatively differing resistance levels via RNA-Seq. This offered unprecedented insights into transcriptional changes associated with host disease resistance. In *U. maydis,* we found effector genes being expressed in a host genotype-dependent manner and for one effector, CRISPR-Cas9-mediated mutagenesis identified a maize line-specific virulence function.

RESULTS

Ustilago maydis disease development in different maize lines

To investigate QDR in the maize–*U. maydis* interaction, we evaluated the susceptibility of different maize lines to *U. maydis* infection. *Ustilago maydis* resistance levels were assessed in the 26 inbred founder lines of the Nested Association Mapping (NAM) recombinant inbred lines (RILs) (McMullen *et al.*, 2009; Yu *et al.*, 2008), a set of maize

lines selected to represent worldwide maize diversity. In addition, the sweet corn Early Golden Bantam (EGB) was used, which is commonly used in *U. maydis* research (Zuo *et al.*, 2019). Seedling infections were performed in three independent biological replicates under controlled conditions with an average of 102 plants per line being scored for *U. maydis* disease symptoms (Figure 1a). In this experimental setup, resistance levels were highly diverse and ranged from very susceptible to very resistant (>94% versus <35% tumours, respectively), while no maize line showed complete resistance to *U. maydis* infection (Figure 1a). Agglomerative hierarchical clustering of disease indices as a measure of *U. maydis* infection severity identified five susceptibility groups (Figure 1b). Two groups consisted only of the most resistant line CML322 and of the most susceptible line Tx303, respectively, and three groups were of comparable sizes, indicating a mostly even distribution of *U. maydis* resistance levels within the NAM founder lines and EGB. The *U. maydis* SG200 strain used in this study was derived from a field isolate from a temperate region (Minnesota, USA; Kämper *et al.*, 2006). Strikingly, among the maize lines with highest susceptibility, most were local to regions close to the origin of SG200 (e.g. Oh43 from Ohio, Mo18w from Missouri, Il14H from Illinois). In contrast, all four most resistant maize lines were of tropical origin (CML322, NC350, NC358, Ki3). Thus, maize lines of close provenance to SG200 were generally more susceptible, indicating a possible adaptation of the local *U. maydis* strain to the local host lines. From each group, one to two lines were chosen based on resistance level, provenance, growth soundness and seed production for subsequent investigations (CML322, B73, EGB, Ky21, Oh43 and Tx303).

To further characterise disease progression of *U. maydis* within the different maize lines and to select a time point suitable for transcriptome analysis, we assessed relative fungal biomass by quantitative PCR (qPCR) using genomic DNA (Figure 1c) and visualised fungal growth within leaf tissue by WGA-AF488/propidium iodide co-staining throughout the infection process at 1, 3, 6 and 9 days post-infection (dpi) (Figure S1).

At 1 and 3 dpi, relative fungal biomass did not differ significantly between the maize lines. At 6 dpi, however, fungal biomass in Tx303, the most susceptible maize line, was increased approximately twofold compared to the other maize lines. In line with previous observations, relative fungal biomass decreased at the late infection time point (9 dpi), which might be due to impaired teliospore formation in the genetically engineered haploid SG200 strain (Lanver *et al.*, 2018). At the microscopic level, the infection progress was comparable for 1 and 3 dpi in all maize lines. At 6 dpi, strong differences could be observed, as for CML322, the most resistant maize line, hyphae were mostly proliferating similarly to earlier stages, whereas for the more susceptible maize lines fungal aggregates, fragmented hyphae and enlarged maize cells were visible (Figure S1). Size and number of fungal aggregates and maize cell enlargements increased with susceptibility levels of the maize lines. Based on these fungal quantification and microscopic growth data, the 3 dpi time point was chosen for transcriptome analysis. At this time point, the different maize lines showed comparable growth of biotrophic hyphae while levels of fungal colonisation allowed sufficient coverage of *U. maydis* genes by RNA-Seq.

Transcriptome analysis of *U. maydis* infecting maize lines of distinct disease resistance levels

For gene expression analysis, maize seedlings of maize lines CML322, B73, EGB, Ky21, Oh43 and Tx303 were infected with *U. maydis* SG200 and water (mock control). Infected and mock-treated leaf sections were collected 3 dpi in biological triplicates and their transcriptome was subsequently analysed via RNA-Seq. After filtering for low expression, 6284 of 6766 *U. maydis* genes remained for the analysis and were considered to be expressed in our samples (93%). To evaluate variability between the samples, we made a multidimensional scaling (MDS) plot (Figure 2a). To additionally examine whether the infection stage in the different maize lines was comparable and to demonstrate that gene expression differences were not caused by faster infection progression in the more susceptible maize lines, we included transcriptome data previously published by Lanver *et al.* (2018), where the maize line EGB was infected with the mixture of the two compatible *U. maydis* wild-type strains FB1 and FB2, and the fungal transcriptome was mapped during different stages of the infection process. All our samples clustered with the 2 dpi samples of Lanver *et al.* (2018), which likely reflects the slower disease progression of SG200 compared to FB1xFB2. Again, this showed no pronounced differences in infection progression between the different maize lines at the time point tested.

To analyse whether *U. maydis* gene expression is influenced by the colonised maize line, we compared expression in all 15 possible pairs of the six different maize lines. This identified in total 406 of the 6284 expressed genes (6.4%) being differentially expressed ($\log_2$(expression fold change) > 0.5, adjusted P value < 0.05, Data Set S1) in at least one of the 15 comparisons. The number of differentially expressed *U. maydis* genes (DEGs) ranged from zero to 300 genes in the different comparisons and only a few genes were differentially expressed in several of the 15 comparisons (Figure 2b,c). The majority of DEGs were only differentially expressed in one to three comparisons (approximately 75%) and only 1% of DEGs was differentially expressed in more than half of the comparisons, reflecting diverse gene expression changes among different maize lines. Strikingly, amongst the 406 DEGs, 102 encode

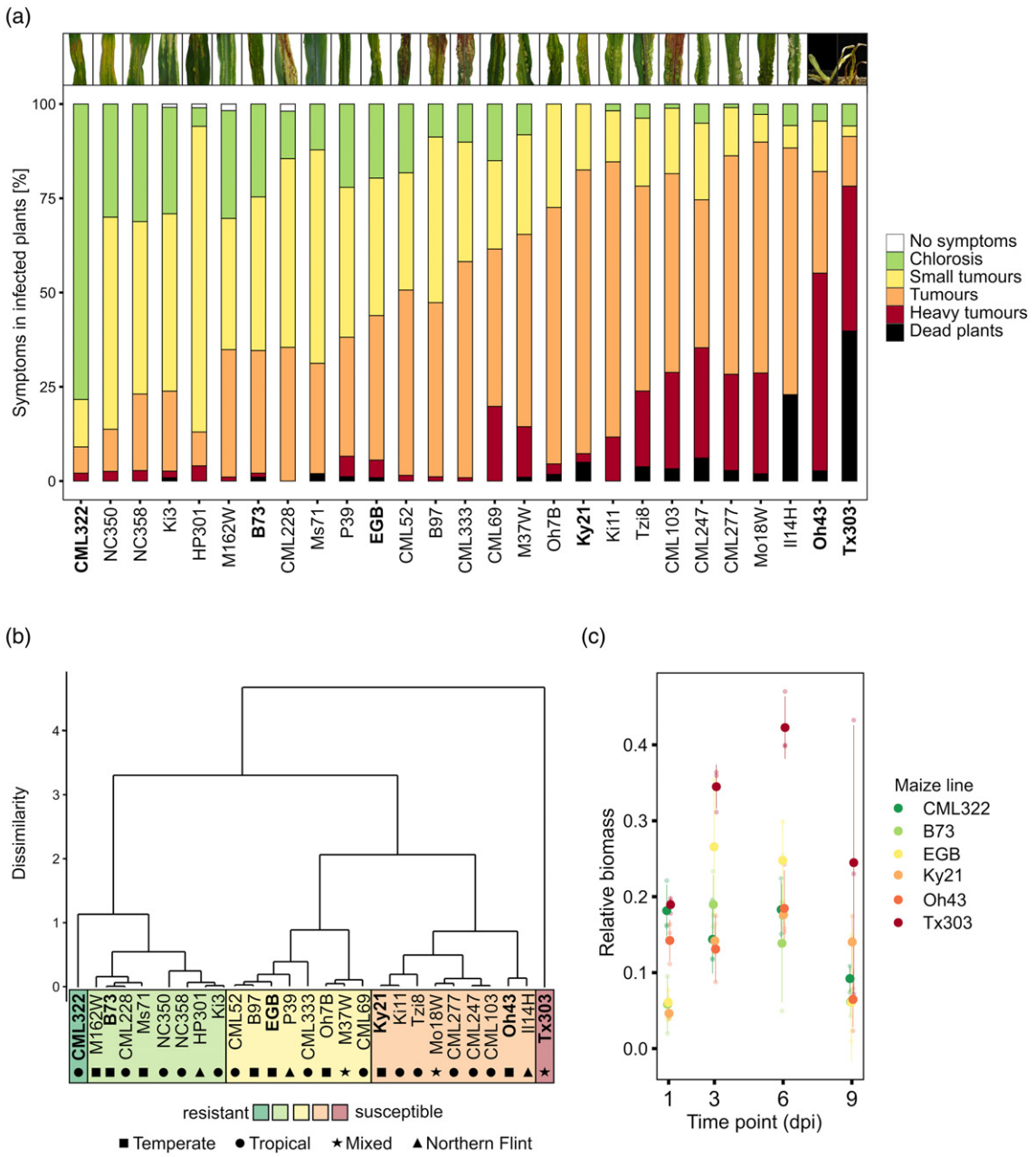

Figure 1. *Ustilago maydis* disease development in the 26 maize NAM founder lines and EGB.
(a) Disease symptom classification. Maize seedlings were infected with *U. maydis* SG200 at the three-leaf stage. Three independent experiments were performed and the average values are expressed as the percentage of the total number of infected plants. Disease symptom classification was done 12 days post-infection (dpi) as described in Redkar and Doehlemann (2016). Average number of infected plants per line: 102. Maize lines selected for RNA-Seq are highlighted in bold. Representative pictures of infected leaves at 12 dpi for each maize line are given at the top.
(b) Agglomerative hierarchical clustering of disease indices. Clustering is based on Euclidean distances of disease indices using complete linkage clustering. Maize lines selected for RNA-Seq are highlighted in bold. The maize lines' provenances are depicted by black symbols.
(c) Fungal biomass quantification based on the amount of genomic DNA. A qPCR with plant-specific (*GAPDH*) and fungus-specific (*ppi*) primers was performed at 1, 3, 6 and 9 dpi in the maize lines selected for RNA-Seq. Solid points give mean ratios of fungal DNA to plant DNA ($2^{-\Delta\Delta Ct}$) of three biological replicates, transparent points give individual values and error bars denote the standard deviation.

candidate secreted effector proteins (CSEPs, Dutheil *et al.*, 2016), which represents a significant 3.3-fold enrichment (hypergeometric *P* value = 5.65e−30) (Figure 2d). Most of these CSEPs do not contain any predicted functional domains (68%). A heatmap based on expression profiles of the 102 line-specific CSEPs shows distinct groups of CSEPs with similar expression patterns (Figure 2e, Data Set S2). Of the 102 CSEPs, one group of 38 genes is upregulated in

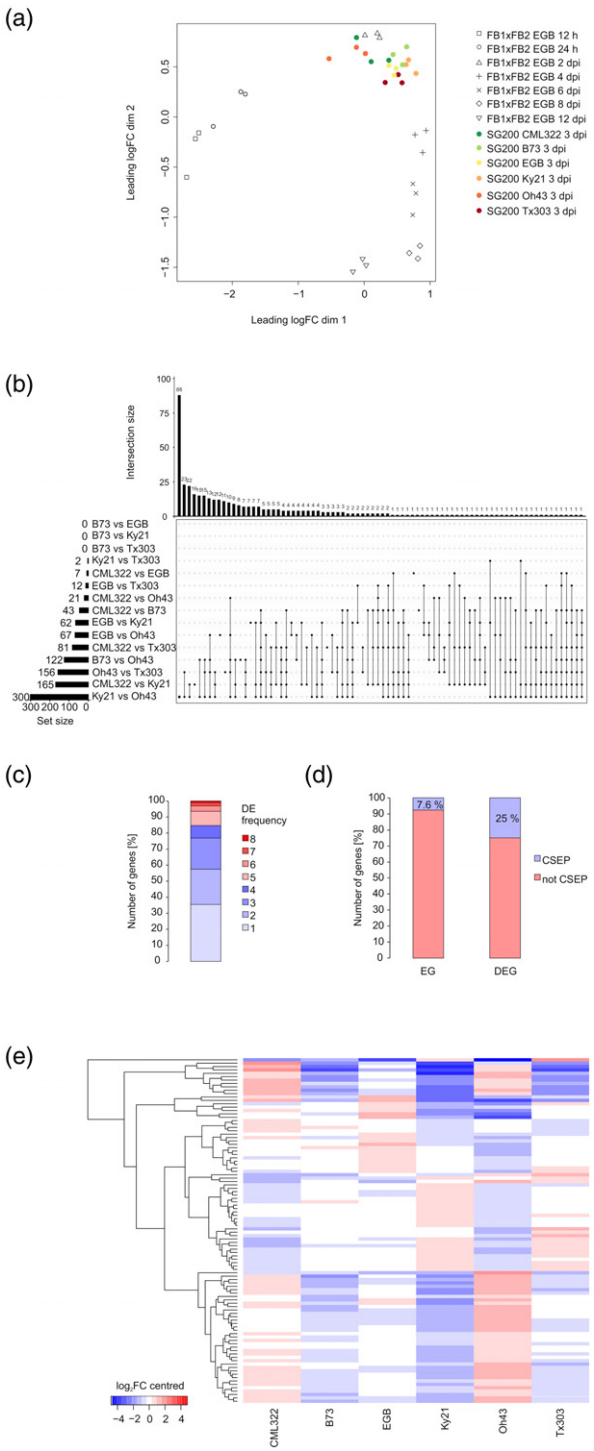

Figure 2. RNA-Seq analysis of *Ustilago maydis* infecting maize lines of differing disease resistances.

(a) MDS plot of *U. maydis* RNA-Seq data. The top 1000 variable genes were used to calculate pairwise distances between the samples. FB1xFB2 RNA-Seq data were previously published and represent different time points in the *U. maydis* disease cycle in EGB (Lanver *et al.*, 2018). MDS: multidimensional scaling.

(b) UpSet plot of the distribution of differentially expressed *U. maydis* genes across maize lines. Genes with $\log_2$(expression fold change) > 0.5 and adjusted *P* value < 0.05 were considered differentially expressed. In total, 406 of 6284 expressed genes were differentially expressed between maize genotypes. The number of differentially expressed genes (DEGs) for each of the 15 possible comparisons is given by set size (horizontal bars). Overlaps of DEGs between comparisons are depicted by connected black dots. DEGs unique to one of the comparisons are depicted by individual black dots. The extent of overlap is shown by intersection size (vertical bars).

(c) Number of differentially expressed genes by frequency of differential expression within comparisons. The categories of the bar plot give the percentage of all DEGs that are differentially expressed in the indicated number of comparisons. DE: differential expression.

(d) Enrichment of CSEPs in differentially expressed genes. Portion of CSEPs in all 6284 expressed *U. maydis* genes compared to the portion of CSEPs in DEGs between maize genotypes. Within DEGs, CSEPs show a 3.3-fold enrichment (hypergeometric test, *P* value = 5.65e−30). EG: expressed gene. DEG: differentially expressed gene. CSEP: candidate secreted effector protein.

(e) Expression profile of differentially expressed *U. maydis* CSEPs across maize lines. The heatmap shows $\log_2$(expression fold change) values compared to mean expression across all samples. CSEP: candidate secreted effector protein.

the most resistant maize line CML322 and downregulated in more susceptible maize lines, except for Oh43, while another group of 29 CSEPs shows an opposite expression pattern. Besides these two main expression patterns, some CSEPs show no clear correlation to the resistance level. Consequently, no dominant expression pattern that underlies all maize line-specific CSEPs was observed.

Weighted gene co-expression network analysis of *U. maydis* genes during infection of maize lines of distinct disease resistance levels

Next, we assessed the correlation of *U. maydis* gene expression with the maize resistance levels. A weighted gene co-expression network analysis (WGCNA) identifies modules of co-expressed genes and represents the modules by summary expression profiles, referred to as the module eigengene (Langfelder and Horvath, 2008; Zhang and Horvath, 2005). This analysis identified 11 colour-coded modules with differential expression profiles of the module eigengenes, ranging in size from 1073 ('turquoise') to 65 genes ('purple') (Figure 3a, Data Set S3). Subsequently, the correlation of each module eigengene with the disease indices of the different maize lines was calculated (referred to as gene significance [GS]) (Figure 3b). The 'purple' module showed a significant positive correlation (GS > 0.5, *P* < 0.05) and the 'greenyellow' module showed a significant negative correlation to the disease index (GS < −0.5, *P* < 0.05), i.e. expression of genes in the 'purple' module is higher in more susceptible maize lines and expression of genes in the 'greenyellow' module is higher in more resistant maize lines. To evaluate which biological processes were associated with the colonisation of more resistant and more susceptible maize lines, the 'purple'

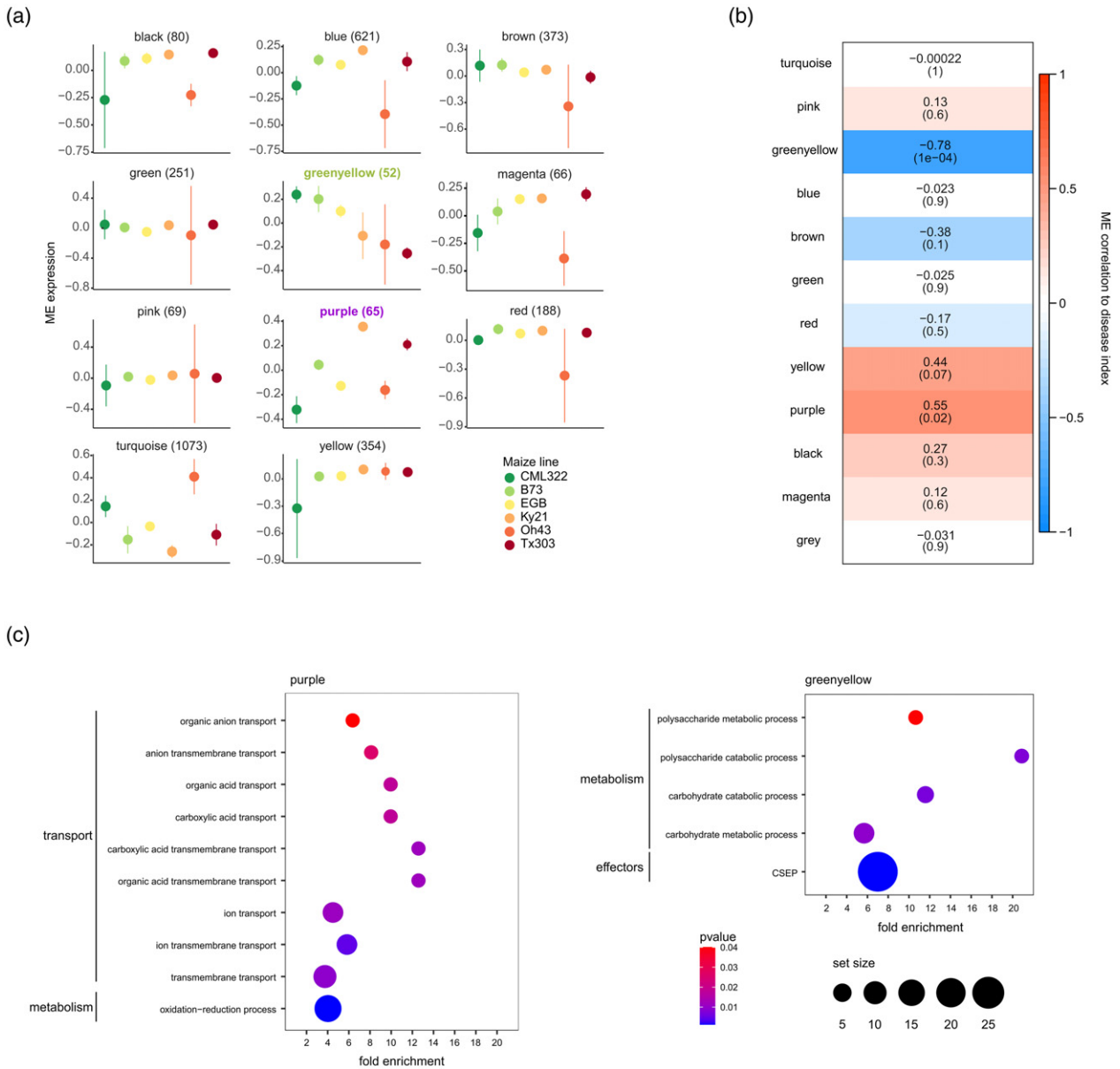

Figure 3. Weighted gene co-expression analysis (WGCNA) of *Ustilago maydis* genes during infection of maize lines of differing disease resistances.
(a) Modules of co-expressed *U. maydis* genes across maize lines. The RNA-Seq data were subjected to WGCNA to detect modules of co-expressed genes. Each plot represents the expression profile of the module eigengene, which can be considered as representative of the expression of the respective co-expression module. Error bars indicate standard deviation of three biological replicates. The modules are named according to their colour, and the size of each module is given in parentheses. Modules significantly correlated with disease index are highlighted in bold and their respective colour.
(b) Module–disease index association. Correlation of modules of co-expressed genes with the disease index of the colonised maize line. Numbers in the heat-map show the correlations with disease index and *P* values in parentheses for the respective module eigengene (ME). Correlation was considered significant if correlation > 0.5 or < −0.5 and $P < 0.05$.
(c) GO and CSEP enrichments in modules correlated with disease index. GO biological process terms and additionally candidate secreted effector proteins (CSEPs) were tested for significant enrichment in the purple (positive correlation to disease index) and greenyellow (negative correlation to disease index) modules. Gene sets were considered significantly enriched if $P < 0.05$ (hypergeometric test). Dot size is representative of the number of analysed genes in the respective term. Only genes with a gene significance to disease index of >0.5 (purple) or <−0.5 (greenyellow) and $P < 0.05$ were considered for the analysis and only terms with a set size of ≥2 are shown.

and 'greenyellow' modules were subjected to enrichment analysis of Gene Ontology (GO) terms and CSEPs (Ashburner *et al.*, 2000; The Gene Ontology Consortium, 2017), (Figure 3c, Data Sets S4, S5). In summary, mostly ion transport processes were significantly enriched in the 'purple' module, which might suggest that different availability of nutrients in more resistant versus more susceptible maize lines could be involved in QDR to *U. maydis*.

Additionally, 'oxidation-reduction' was the GO term with the most genes. Oxidation-reduction processes are involved in metabolism as well, but can also have a signalling function or be related to detoxification of reactive oxygen species. In the 'greenyellow' module, all significantly enriched GO terms were related to carbohydrate metabolism. In addition, CSEPs were significantly enriched in this module and represented the biggest category which might reflect an elevated need for the fungus to suppress enhanced defence mechanisms in more resistant host lines.

Transcriptome analysis of *U. maydis*-infected maize lines of distinct disease resistance levels

To identify maize genes involved in QDR to *U. maydis,* we analysed genotype-dependent transcriptional changes in response to *U. maydis* via RNA-Seq. Of all 63 477 maize annotated loci, 40 056 were expressed in our samples (63%). To assess the variability between the samples we used an MDS plot (Figure 4a). *Ustilago maydis*-infected and control samples formed two distinct groups, within which the samples of each maize line clustered together, indicating both treatment-specific and genotype-specific expression patterns. We compared expression fold changes of the *U. maydis*-infected samples to the respective control samples for all 15 possible pairs of six different maize lines (i.e. difference between genotypes in response to infection). This analysis showed that in total 8675 of 40 056 transcripts (22%) responded differentially to *U. maydis* infection ($\log_2$(expression fold change) > 0.5, adjusted *P* value < 0.05, Data Set S6) in at least one of the 15 comparisons. The number of DEGs ranged from 358 to 1283 genes in the different comparisons and the fraction of genes differentially expressed in several of the 15 comparisons was very small (Figure 4b). Around 50% of DEGs were differentially expressed in only one of the comparisons and only 4% of DEGs were differentially expressed in more than half of the comparisons. Together, this shows that genes differentially responding to *U. maydis* infection are highly diverse between maize lines.

To identify biological processes which were associated with the maize line-specific gene expression responses, all DEGs were subjected to enrichment analysis of GO terms (Ashburner *et al.*, 2000; The Gene Ontology Consortium, 2017), highlighting processes involved in transport, response to stimulus, cellular processes and metabolism (Figure 4d, Data Set S8). The GO terms with most genes were 'transmembrane transport', 'oxidation-reduction' and 'protein phosphorylation', which could indicate a special importance of these processes in DEGs in response to *U. maydis* between maize lines. Transport processes play a pivotal role in signalling and nutrient uptake, as well as growth and development. Oxidation-reduction processes are involved in metabolism but can also have a signalling function. Protein phosphorylation occurs during kinase signalling processes. A predominant role of genes related to metabolism as well as kinase signalling cascades for QDR has been proposed before (Delplace *et al.*, 2020). Together, this suggests that maize line-specific responses to *U. maydis* involve various cellular activities, consistent with the complex nature of QDR. To examine if the maize DEGs include genes associated with other forms of immunity, we compared *Arabidopsis thaliana* orthologues of the DEGs with *A. thaliana* genes previously found to be linked to pathogen-associated molecular pattern (PAMP)-triggered immunity (PTI) and/or effector-triggered immunity (ETI) responses (Dong *et al.*, 2015; Hatsugai *et al.*, 2017; Mine *et al.*, 2018). However, of the 3264 DEG *A. thaliana* orthologues, only about 11% (363 and 360 genes) were found in common with either ETI- and/or PTI-associated genes (Figure S2a).

To assess which processes were connected to *U. maydis* resistance or susceptibility, the correlation of expression changes between *U. maydis* infection and mock treatment of each gene of the respective maize line to the disease index was calculated (Data Set S7). All DEGs were then filtered for genes with a significant positive (GS > 0.5 and *P* < 0.05, Figure 5a) or negative (GS < −0.5 and *P* < 0.05, Figure 5b) correlation to the disease index. These two sets of genes were again subjected to enrichment analysis of GO terms (Figure 5a,b, Data Sets S9, S10). In the DEGs with positive correlation to the disease index, i.e. upregulated in more susceptible maize lines, enrichments were found in four main cellular activities: cellular processes, response to stimulus, transport and metabolism (Figure 5a). The enriched GO term with the largest number of genes was 'protein phosphorylation', one of the most important cellular regulatory mechanisms involved in signal transduction. Furthermore, biological process terms that can be linked to cell division processes ('DNA replication', 'microtubule-based movement') and 'sexual reproduction'/'recognition of pollen' were significantly enriched. In DEGs negatively correlated to the disease index, i.e. genes upregulated in the more resistant maize lines, enrichments were found in transport and metabolism (Figure 5b). The enriched GO term with the largest number of genes was 'translation', and a process that could be involved in photosynthesis ('porphyrin-containing compound biosynthetic process') was most strongly enriched.

Identification of maize line-specific *U. maydis* effectors

As *U. maydis* genes encoding CSEPs were enriched both in genes differentially expressed between maize lines and in the co-expression module correlated to infection severity, we investigated whether line-specifically expressed CSEPs also have line-specific functions for virulence. Twelve candidate maize line-specific CSEP genes were selected from all 102 differentially expressed CSEPs based

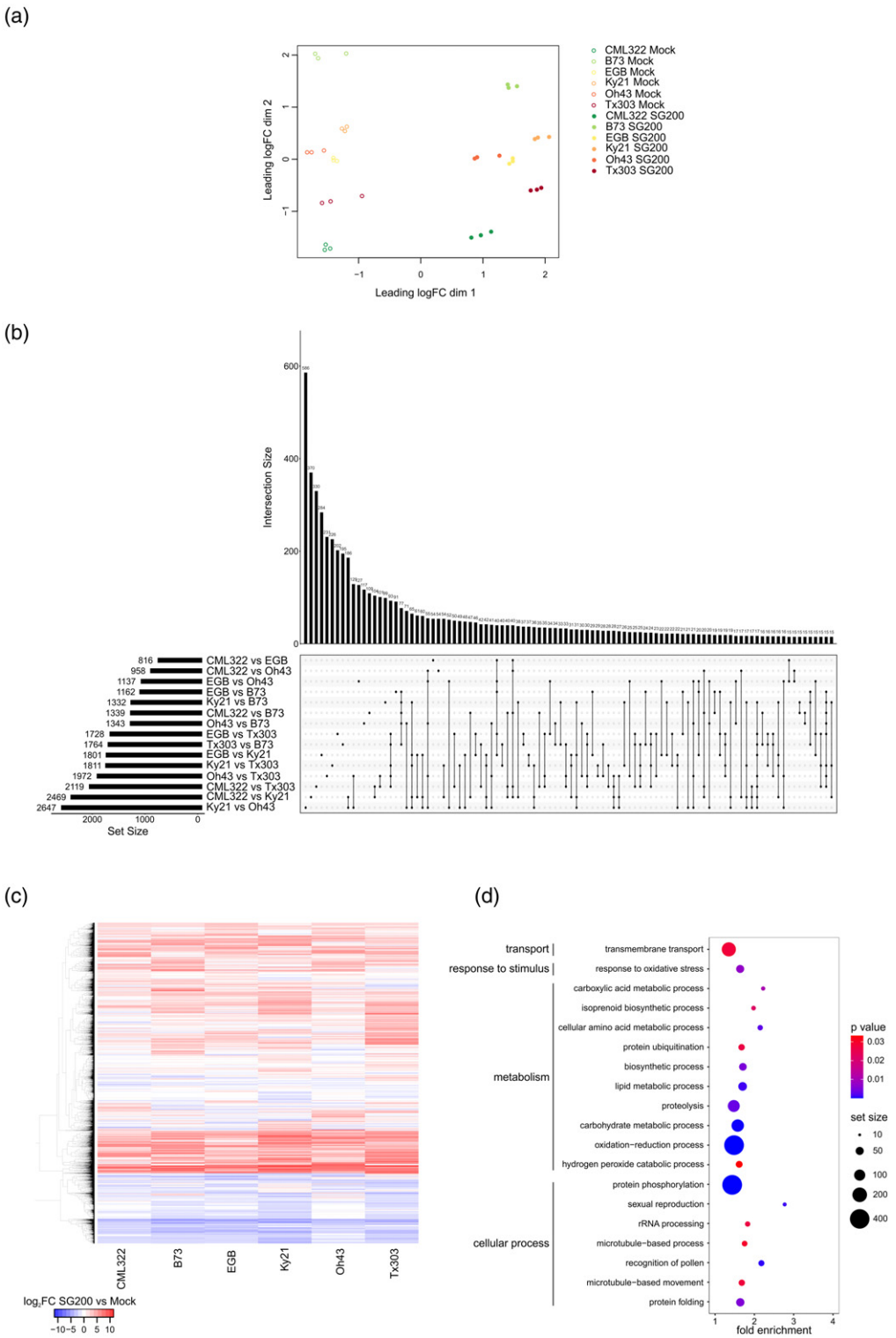

on a high log_2 (expression fold change) value and an expression pattern with higher expression in resistant and lower expression in susceptible maize lines or vice versa (sum of log_2 (expression fold change) across all samples >2; Figure 6a). CSEPs with similar expression patterns were targeted for simultaneous knock-out (KO) in the

Figure 4. RNA-Seq analysis of maize gene expression in response to *Ustilago maydis*.
(a) MDS plot of maize RNA-Seq data. The top 5000 variable genes were used to calculate pairwise distances between the samples. MDS: multidimensional scaling.
(b) UpSet plot of the distribution of differentially expressed genes (DEGs) between maize lines in response to *U. maydis*. Genes with $\log_2$(expression fold change) > 0.5 of the gene expression changes and adjusted *P* value < 0.05 were considered differentially expressed (difference between genotypes in response to infection). In total, 8675 of 40 056 expressed genes responded differentially to *U. maydis* between maize genotypes. The number of DEGs for each of the 15 possible comparisons is given by set size (horizontal bars). Overlaps of DEGs between comparisons are depicted by connected black dots. DEGs unique to one of the comparisons are depicted by individual black dots. The extent of overlap is shown by intersection size (vertical bars).
(c) Expression profile of differentially expressed maize genes in response to *U. maydis*. The heatmap shows $\log_2$(expression fold change) values of SG200-infected versus mock-treated samples.
(d) GO enrichments in differentially expressed maize genes. GO biological process terms were tested for significant enrichment in all DEGs between maize lines in response to *U. maydis*. Gene sets were considered significantly enriched for *P* < 0.05 (hypergeometric test). Dot size is representative of the number of analysed genes in the respective term. Only terms with a set size of ≥10 are shown.

SG200 background using the CRISPR/Cas9 system, generating frameshift mutations near the 5′ ends of the respective genes (Figure 6a,b, Data Set S13, Schuster *et al.*, 2016). Plant infections with the generated *U. maydis* mutant strains identified line-specific virulence functions for the CSEP genes UMAG_02297 and/or UMAG_05027 (Figure 6c). While virulence of the double mutant KO_UMAG_02297/KO_UMAG_05027 was not reduced on B73 or EGB, a significant reduction was observed on CML322 and Oh43. For reasons of seed availability, subsequent analyses of the mutants were focused on the maize line CML322. Here, the virulence defect could be restored by introducing single copies of both genes into the *ip* locus of the double mutant strain, demonstrating specificity of the observed virulence reduction (Figure 6c).

To assess if both or only one of the genes contribute to maize line-specific virulence of KO_UMAG_05027/KO_UMAG_02297 on CML322, single KO mutants of UMAG_02297 and UMAG_05027 were tested for virulence on EGB and CML322. This showed that UMAG_02297 alone, but not UMAG_05027, was necessary for full virulence on CML322. The virulence defect of KO_UMAG_02297 could be restored by introducing a single copy of UMAG_02297 into the *ip* locus of the mutant strain (Figure 6c). In addition, a line-specific virulence function was observed for UMAG_05318 and/or UMAG_11416 (Figure S4). Here, the double mutant KO_UMAG_05318/KO_UMAG_11416 showed reduced virulence on EGB, but not B73. As the single KO strain KO_UMAG_11416 did not show any virulence defect (Figure S5) and a reduction of virulence for a UMAG_05318 deletion strain had already been reported previously (Schilling *et al.*, 2014), these CSEPs were not further investigated. For all other tested mutants, either no reduction of virulence or a reduction of virulence on all tested maize lines was observed (Figure S4).

Relative expression levels of UMAG_02297 were analysed via quantitative reverse transcriptase-PCR (qRT-PCR) on the six different maize lines (Figure S3b). Interestingly, UMAG_02297 was expressed at the lowest levels on CML322 throughout the infection process, the maize line on which it was required for full virulence. Hence, high expression levels do not seem to determine the function for virulence. To investigate the relation of expression level of the effector and *U. maydis* virulence, we generated a strain in which UMAG_02297 was expressed under control of the promoter ppit2, which is highly active throughout the infection process and results in strong overexpression of the gene (Mueller *et al.*, 2013). EGB and CML322 seedlings were infected with Ppit2:UMAG_02297 single and multiple integration strains (Figure 6d). Interestingly, the overexpression strain showed a maize line-specific virulence defect as well: on CML322, but not on EGB, the multiple integration strain was significantly reduced in virulence compared to strain SG200. This shows that a fine-tuned expression of UMAG_02297 is required for virulence on maize line CML322.

Host transcriptional changes induced by UMAG_02297

To investigate which host processes might be influenced by the maize line-specific effector UMAG_02297, leaf samples of CML322 maize seedlings infected with SG200 and KO_UMAG_02297 were analysed by RNA-Seq at 3 dpi. Of all 63 477 maize annotated loci, 30 637 were expressed in these samples (48%). To assess variability between the samples, we made an MDS plot (Figure 7a). Both *U. maydis*-infected samples formed one cluster highly distinct from the mock-treated samples, indicating that maize gene expression was mostly influenced by infection in general, rather than by the different *U. maydis* strains.

To identify genes which were uniquely responsive to infection with SG200 or the UMAG_02297 KO strain, we compared expression levels between the infected samples and the CML322 mock sample ($\log_2$(expression fold change) > 0.5, adjusted *P* value < 0.05, Data Set S11). Overall, the number of DEGs in response to the KO strain was similar to that upon SG200 infection (SG200: 6046 genes upregulated and 3646 genes downregulated compared to mock; KO strain: 5699 genes upregulated and 3212 genes downregulated compared to mock). Most of the DEGs were jointly regulated: 91% of the upregulated genes (5486) and 81% of the downregulated genes (2962) were equivalently regulated in response to both strains. Only

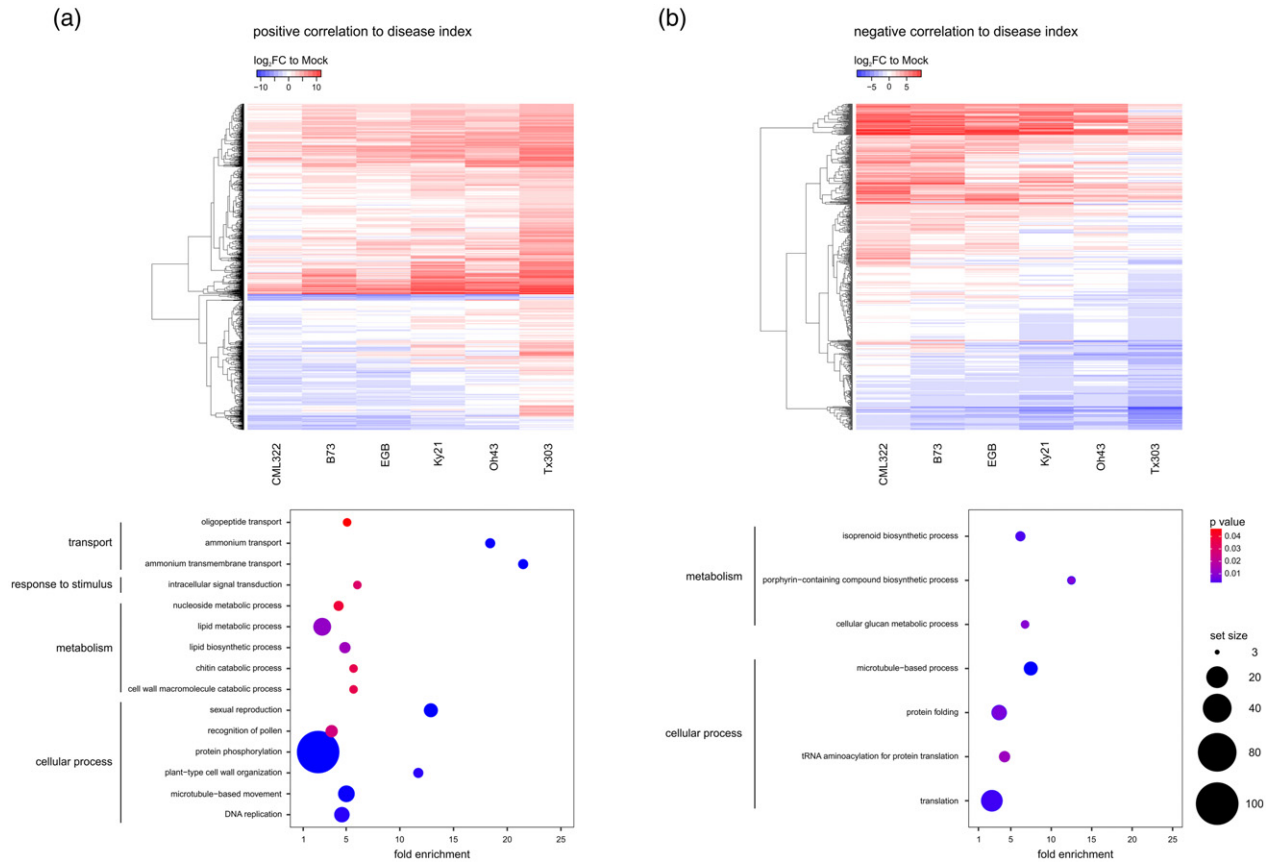

Figure 5. Correlation of maize gene expression to *Ustilago maydis* resistance levels.
(a) Expression profile and enrichments of genes positively correlated with the disease index. Genes with a gene significance for the disease index of >0.5 and $P < 0.05$ were considered to be significantly positively correlated to the disease index. The heatmap shows $\log_2$(expression fold change) values of SG200-infected versus mock-treated samples. GO biological process terms were tested for significant enrichment in all DEGs between maize lines in response to *U. maydis* that were positively correlated to the disease index. Gene sets were considered significantly enriched for $P < 0.05$ (hypergeometric test). Dot size is representative of the number of analysed genes in the respective term. Only terms with a set size of ≥3 are shown.
(b) Expression profile and enrichments of genes negatively correlated with the disease index. Genes with a gene significance for the disease index of <−0.5 and $P < 0.05$ were considered to be significantly negatively correlated to the disease index. The heatmap shows $\log_2$(expression fold change) values of SG200-infected versus mock-treated samples. GO biological process terms were tested for significant enrichment in all DEGs between maize lines in response to *U. maydis* that were negatively correlated to the disease index. Gene sets were considered significantly enriched for $P < 0.05$ (hypergeometric test). Dot size is representative of the number of analysed genes in the respective term. Only terms with a set size of ≥3 are shown.

around 9% and 4% (560 and 213 genes) were uniquely upregulated in response to SG200 or KO, respectively, and around 19% and 8% (684 and 250 genes) were uniquely downregulated in response to SG200 or KO, respectively. Taken together, this indicates that maize gene expression is slightly and specifically altered by UMAG_02297. To gain insight into which host processes could be targeted by UMAG_02297, genes uniquely responsive to each of the strains were additionally filtered for genes that were differentially expressed in response to *U. maydis* SG200 infection between CML322 and EGB, where UMAG_02297 was not found to have a function for virulence (426 genes). Within these, genes predicted to encode auxin efflux transporters were strongly enriched (12-fold enrichment, hypergeometric $P = 0.002$, Data Set S12). Interestingly, we additionally found several other genes predicted to be related to auxin (Figure 7c). The auxin efflux carrier pin12 (GRMZM2G160496_P01) and auxin-responsive SAUR32 (GRMZM2G466229_P01) were similarly regulated in CML322 in response to KO and in EGB in response to SG200, while SAUR56 (GRMZM2G414727_P01) and the auxin efflux carrier PIN5a (GRMZM2G025742_P01) differed more strongly between the maize lines (SG200- and KO-infected CML322 versus SG200-infected EGB). This observed specific regulation of auxin-related genes identifies the manipulation of the auxin pathway as a potential maize line-specific target of UMAG_02297.

DISCUSSION

Our plant inoculation experiments revealed that *U. maydis* resistance levels of the NAM founder lines and EGB are highly diverse, which further corroborates the quantitative

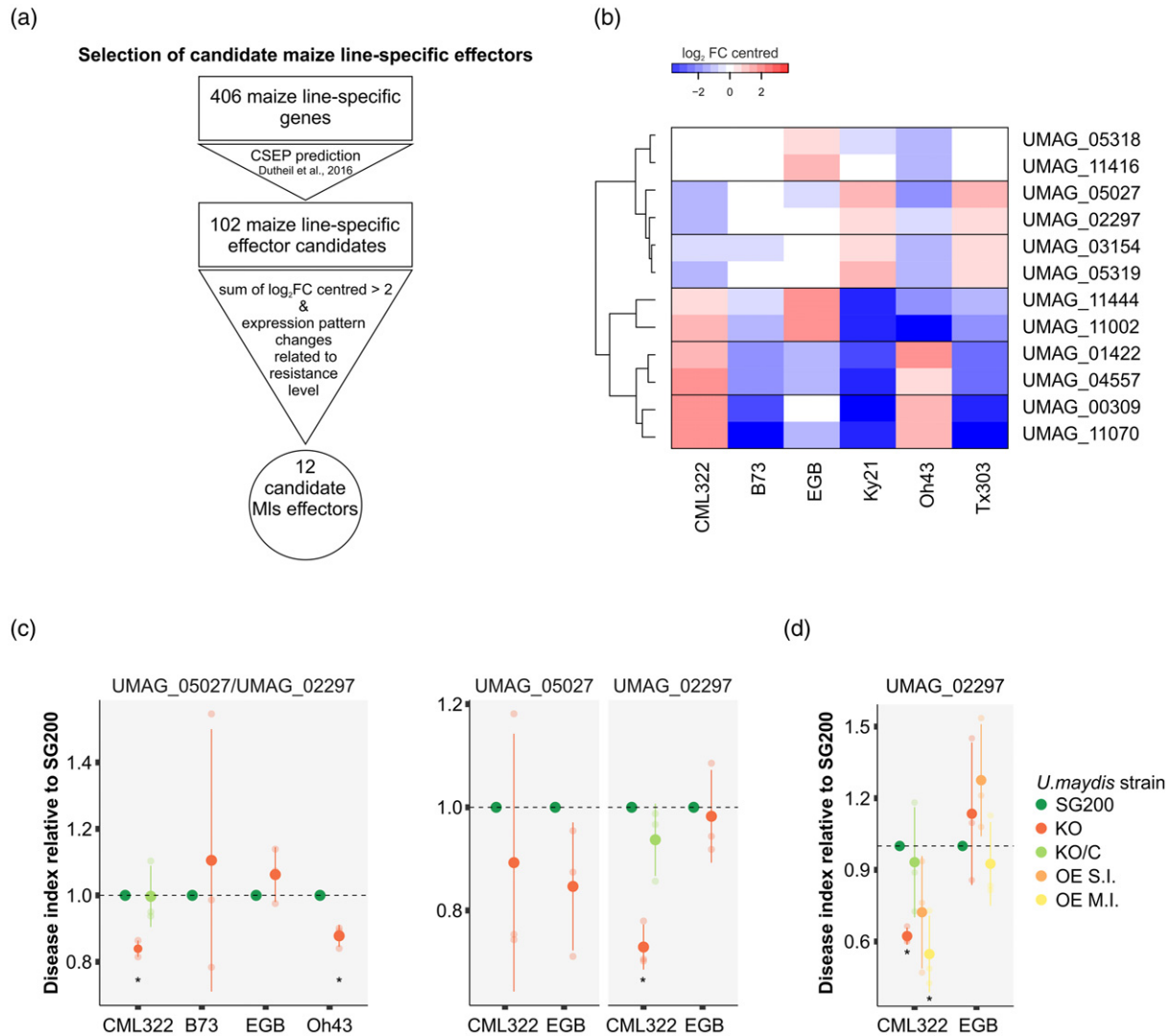

Figure 6. Expression pattern and virulence function of candidate maize line-specific effectors.
(a) Selection of maize line-specific effector candidates for functional characterization.
(b) Expression profile of selected maize line-specific effector candidates across maize lines. The heatmap shows $\log_2$(expression fold change) values compared to mean expression across all samples.
(c) Virulence function of candidate maize line-specific effectors. Double and single knock-out (KO) mutant strains of selected maize line-specific effectors were injected into maize seedlings of the indicated line and symptoms were scored 12 days post-infection (dpi). Gene names are given at the top. KO refers to the respective CRISPR/Cas9 knock-out strain. Gene names separated by a slash indicate double KO of these genes. KO/C indicates that a single copy of the respective gene(s) was introduced into the KO strain for complementation. Disease indices reflect disease symptom severity and are shown in relation to SG200, which was set to unity. Asterisks indicate a significant reduction in disease index compared to SG200 (Student's *t*-test, $P < 0.05$). All experiments were performed in three independent biological replicates. Average number of infected plants per strain and maize line: 89.
(d) Impact of UMAG_02297 overexpression on virulence. SG200, KO_UMAG_02297, KO_UMAG_02297/C and OE_UMAG_02297 strains were injected into CML322 and EGB seedlings and symptoms were scored 12 dpi. OE: overexpression. S.I.: single integration. M.I.: multiple integration. Disease indices reflect disease symptom severity and are shown in relation to SG200, which was set to unity. Asterisks indicate a significant reduction in disease index compared to SG200 (Student's *t*-test, $P < 0.05$). All experiments were performed in three independent biological replicates. Average number of infected plants per strain and maize line: 86.

nature of the *U. maydis*–maize interaction. The transcriptome analysis of six *U. maydis*-infected maize lines of different resistance levels offered unprecedented insights into the transcriptional changes associated with host disease resistance. Resistance levels of the NAM founder lines to other diseases such as northern corn leaf blight or aphids have been previously analysed, which revealed distinct patterns from the *U. maydis* resistance levels observed in this study. B73 for example is highly susceptible to northern corn leaf blight, while CML322 is very resistant and Ky21, Oh43 and Tx303 showed medium susceptibility levels (Poland *et al.*, 2011). Aphid resistance

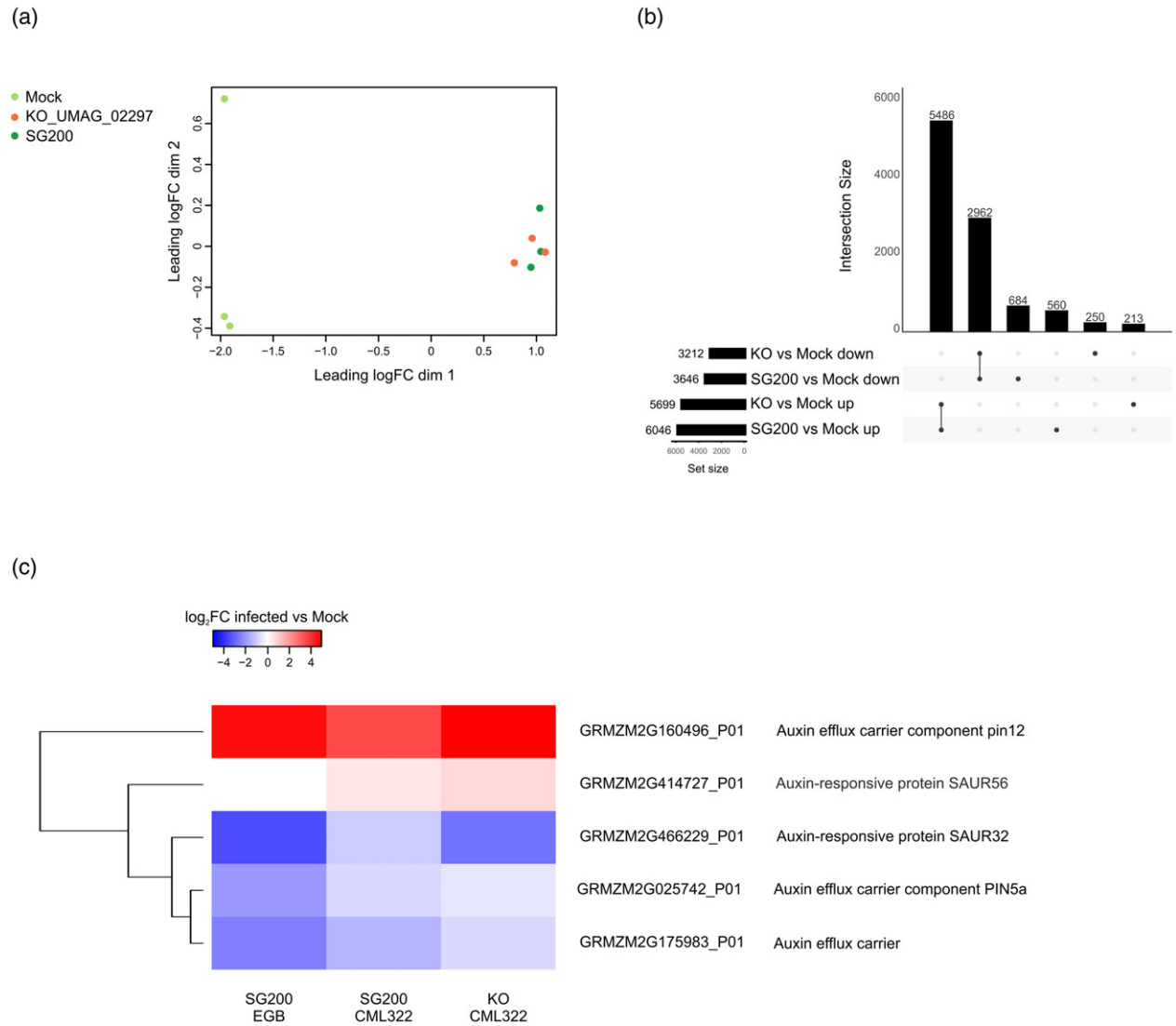

Figure 7. Maize gene expression changes in response to *Ustilago maydis* KO_UMAG_02297. The transcriptome of CML322 maize seedlings infected with SG200, KO_UMAG_02297 and mock was analysed via RNA-Seq 3 days post-infection (dpi). KO: knock-out.
(a) MDS plot of maize RNA-Seq data. The top 5000 variable genes were used to calculate pairwise distances between the samples. MDS: multidimensional scaling.
(b) UpSet plot of maize genes differentially expressed in response to SG200 and KO_UMAG_02297 infections in comparison to mock. Genes with $\log_2$(expression fold change) > 0.5 or < −0.5 and adjusted *P* value < 0.05 were considered differentially expressed. In total, 10 155 of 30 637 expressed genes were differentially expressed. The number of differentially expressed genes (DEGs) for each of the 15 possible comparisons is given by set size (horizontal bars). Overlaps of DEGs between comparisons are depicted by connected black dots. DEGs unique to one of the comparisons are depicted by individual black dots. The extent of overlap is shown by intersection size (vertical bars).
(c) Expression profile of auxin-related maize genes in response to *U. maydis* SG200 and KO_UMAG_02297 in EGB and CML322. The heatmap shows $\log_2$(expression fold change) values of infected versus mock-treated samples.

was found high in Tx303, Oh43 and Ky21, whereas CML322 was found to be highly susceptible and B73 displayed medium aphid susceptibility (Meihls *et al.*, 2013). For *U. maydis*, CML322 displayed the highest resistance levels, followed by B73, and Ky21, Oh43 and Tx303 were moderately to highly susceptible. This suggests that specific, rather than general defence mechanisms determine the outcome of maize interactions with different pathogens and pests.

Maize line-specific gene expression in *U. maydis*

For *U. maydis,* our analysis of genes which were differentially expressed between host genotypes showed a significant enrichment of CSEPs. Additionally, CSEPs were significantly enriched in the co-expression module that was negatively correlated to the disease index, i.e. within genes that were upregulated in the more resistant maize lines. Both these findings indicate a predominant role of

CSEPs in colonising host lines of different resistance levels and point to an important involvement of CSEPs in targeting components of QDR.

In the co-expression module correlated to colonisation of more resistant host lines, enriched biological processes included mechanisms connected to carbohydrate metabolism, which in plant pathogenic fungi has been directly linked to plant cell wall degradation (Ospina-Giraldo *et al.*, 2003; Tonukari *et al.*, 2000). During *U. maydis* infection, degradation of cell walls was previously found to be important at very early stages to allow initial penetration and intracellular growth, as well as in later stages when plant cell walls need to be loosened to enable cell enlargement for tumour formation, rather than being used as a nutrient source (Doehlemann *et al.*, 2008b; Lanver *et al.*, 2018). One could speculate that enhanced cell wall reinforcements or different cell wall compositions might be an additional obstacle the fungus needs to overcome when colonising host lines of higher resistance levels. Several studies have suggested differences in cell wall composition as factors in host–pathogen interactions (Bacete *et al.*, 2020; Vorwerk *et al.*, 2004). *Arabidopsis thaliana* mutants of the GPI-anchored putative pectate lyase PMR6 were found to be highly resistant to powdery mildew (Vogel *et al.*, 2002). In wheat, variation in pectin composition has been associated with resistance to the stem rust fungus *Puccinia graminis* (Wiethölter *et al.*, 2003). In maize, differences in cell wall composition between different lines have been reported (Hazen *et al.*, 2003). A cell wall carbohydrate profiling of all NAM founder lines would allow investigating if more resistant or more susceptible maize lines share similar cell wall compositions and would thereby help to answer the question to which extent natural variation in cell wall composition affects pathogen resistance.

Another functional group of *U. maydis* genes that were correlated to infection of more susceptible lines is linked with ion transport processes. The exchange of nutrients between cells is predominantly driven by an ion gradient which is produced by the activity of plasma membrane H^+-ATPases that transport ions through the membrane (Gianinazzi-Pearson *et al.*, 1991; Palmgren, 1990; Sondergaard *et al.*, 2004; Wang *et al.*, 2014). During mycorrhizal symbiosis, plant H^+-ATPases were found to energise nutrient uptake in rice and *Medicago truncatula* (Wang *et al.*, 2014). *Ustilago maydis* contains two H^+-ATPases that could be involved in nutrient uptake (Robles-Martínez *et al.*, 2013). Together with the previous finding that different nutrient transporters are important virulence factors tied to biotrophic development in *U. maydis* (Lanver *et al.*, 2018; Schuler *et al.*, 2015; Wahl *et al.*, 2010), this could indicate that different availability of nutrients in more resistant versus more susceptible maize lines is involved in QDR to *U. maydis*.

Maize processes involved in QDR against *U. maydis*

To gain insight into the host processes which are involved in QDR to *U. maydis,* we analysed genotype-dependent transcriptional changes in response to *U. maydis* in maize lines of distinct resistance levels. The major functional classes within maize DEGs were related to 'transmembrane transport', 'oxidation-reduction' and 'protein phosphorylation'. Protein phosphorylation through kinases is a central process for signal transduction in immune responses. Interestingly, kinases have been shown to play important roles in QDR in several cases. Two maize wall-associated kinases, ZmWAK-RLK1 and ZmWAK, confer QDR to northern corn leaf blight and a close relative of *U. maydis*, *Sporisorium reilianum*, respectively (Hurni *et al.*, 2015; Zuo *et al.*, 2015). Transport processes are essential for plant responses during interactions with pathogens, and several QDR genes encode putative transporters. For example, the ABC transporter encoded by *Lr34* confers resistance to diverse fungal pathogens in wheat (Krattinger *et al.*, 2009). Hence, this suggests a possible role for kinases as well as transport processes also in QDR against *U. maydis*. Together, our analysis shows that genes associated to QDR to *U. maydis* include genes of various functional classes, in line with the complex nature of QDR and the idea that QDR extends beyond pathogen perception (Corwin and Kliebenstein, 2017). The finding that only a small fraction of the DEGs was shared with genes previously found to be associated with PTI and ETI in *A. thaliana*, assuming conservation of PTI and ETI between maize and *A. thaliana*, implies that QDR mechanisms are mostly distinct from PTI and ETI gene networks (Dong *et al.*, 2015; Hatsugai *et al.*, 2017; Mine *et al.*, 2018).

Correlation analysis of gene expression to resistance levels via WGCNA again identified processes involved in protein phosphorylation, as well as cell division being upregulated in the more susceptible maize lines in response to *U. maydis*. To build a tumour, the fungus actively triggers cell division and reactivates DNA synthesis in the leaf tissue, which goes along with alterations of genes involved in cell cycle regulation (Matei *et al.*, 2018; Redkar *et al.*, 2015; Villajuana-Bonequi *et al.*, 2019). In the *A. thaliana–Plasmodiophora brassicae* interaction, which is also accompanied by gall formation, genes involved in cell proliferation were found to be associated with QDR (Jubault *et al.*, 2013). In addition to the obvious involvement in tumour formation, cell cycle deregulation was also found to have an impact on expression of R genes and can thereby modulate plant defence (Bao *et al.*, 2013). Thus, one could speculate that genes involved in cell division might also play a role in QDR against *U. maydis*.

In the more resistant maize lines, processes involved in photosynthesis were significantly enriched. It was shown previously that *U. maydis* suppresses the induction of

photosynthesis-associated genes in infected leaves (Doehlemann *et al.*, 2008a; Horst *et al.*, 2008). This is accompanied by an increase of free hexose levels and a decrease in chlorophyll content, reflecting that the fungus blocks the transition to a photosynthetically active source tissue (Doehlemann *et al.*, 2008a; Matei *et al.*, 2018). Free hexoses within tumour cells are thought to serve as an easily accessible carbon source for the fungus, as well as help to build up osmotic pressure for tumour cell expansion (Horst *et al.*, 2010; Horst *et al.*, 2008). Infection experiments using maize mutants with distorted starch metabolism showed that alterations in carbon allocation are an important factor influencing *U. maydis* growth and plant defence (Kretschmer *et al.*, 2017). Inefficient suppression of photosynthesis, as found in the more resistant maize lines, might result in changes in carbon allocation as well and consequently lead to a reduction in fungal proliferation. However, based on the available data one cannot exclude the possibility that the positive correlation of photosynthesis repression and fungal infection is a consequence rather than a cause of enhanced susceptibility. Nevertheless, as the developmental stages of the fungus in all our samples were comparable, it is likely that the observed resistance level-specific transcriptional changes directly contribute to the outcome of the quantitative interaction with *U. maydis*.

Maize line-specific activity of *U. maydis* CSEPs

It has been hypothesized that allelic variation between plant genotypes in genes contributing to resistance or susceptibility likely builds the molecular basis of QDR (Niks *et al.*, 2015). This can lead to altered expression patterns or different modes of defence reactions, but also alter the efficiency an effector can interact with and thereby manipulate its respective host target. Therefore, the targets of pathogen effectors which quantitatively contribute to virulence are potential candidates contributing to QDR and thus, the identification of these targets can help to elucidate the diverse genetic basis of QDR. For one *U. maydis* effector, ApB73, a maize line-specific virulence function has been demonstrated as well; however, the differences were only quantitative (Stirnberg and Djamei, 2016). One other example supporting the hypothesis that allelic variations in effector targets may be the basis of QDR came from the comparison of the capacity of the EPIC1 effector from two different *Phytophthora* species to suppress their target RCR3, a papain-like cysteine protease. EPIC1 from *Phytophthora infestans* was able to inhibit RCR3 from tomato (*Solanum lycopersicum*) and potato (*Solanum tuberosum*), but not PmEPIC1 from the non-adapted *Phytophthora mirabilis*. However, PmEPIC1 was highly effective in inhibiting an RCR3-like protease in *Mirabilis jalapa*. These different specificities resulted from single amino acid polymorphisms in both the host target and the pathogen effectors, underpinning the importance of ecological effector diversification (Dong *et al.*, 2014).

In this study, we identified a maize line-specific virulence function for the effector gene UMAG_02297. The unexpected finding that overexpression of UMAG_02297, similar to its KO, resulted in a maize line-specific virulence defect, additionally underlines that manipulation of host processes by effectors requires a fine-tuned adaptation to the host genotype. The analysis of transcriptional changes induced by the UMAG_02297 KO mutant in comparison to wild type infections identified auxin-responsive processes being a possible target of this effector. Maize transcriptional changes in response to another *U. maydis* effector mutant of attenuated virulence, ΔSee1, did not show an enrichment of auxin-related genes (Redkar *et al.*, 2015; Villajuana-Bonequi *et al.*, 2019), suggesting that the observed changes in auxin-related gene expression are specific to the deletion of UMAG_02297 rather than a general consequence of altered virulence. In general, auxins play a cardinal role in controlling plant growth and development. A role for auxin in the cell enlargement of *U. maydis*-induced tumours has been proposed before, as auxin synthesis as well as auxin-responsive genes are transcriptionally induced during tumour development and auxin levels within *U. maydis*-induced tumours are elevated (Doehlemann *et al.*, 2008a; Reineke *et al.*, 2008; Turian and Hamilton, 1960). Additionally, auxin can act as an antagonist of the SA pathway in plant defence, and thereby could promote fungal growth and disease development (Kazan and Manners, 2009). Previous studies have identified a large number of auxin-related genes that underlie QDR. For example, in the soybean–*Phytophthora sojae* interaction, auxin catabolite accumulation differed between a relatively resistant and a more susceptible soybean cultivar, and the ability of resistant cultivars to cope with auxin accumulation was suggested to play an important role in QDR in this pathosystem (Stasko *et al.*, 2020). In maize, cloning of the causal gene of the Gibberella stalk rot resistance QTL *qRfg2* identified ZmAuxRP1, which encodes a plastid stroma-localised auxin-regulated protein, presumably modulating auxin biosynthesis (Ye *et al.*, 2019). Furthermore, increased auxin levels have been generally found to lead to enhanced susceptibility to several biotrophic pathogens (Mutka *et al.*, 2013; Navarro *et al.*, 2006; Wang *et al.*, 2007) and a few pathogen effectors that target auxin-related processes have been identified so far. The *Pseudomonas syringae* effector AvrRpt2 for example initiates auxin signalling through degradation of auxin/indole acetic acid proteins (Cui *et al.*, 2013), and the effector PSE1 from *Phytophthora parasitica* modulates local auxin levels through altered distribution of auxin efflux transporters (Evangelisti *et al.*, 2013). Together, this renders auxin-related processes an interesting and promising possible target of UMAG_02297, which will be tested in future studies.

Together, our study revealed the influence of different host genotypes on *U. maydis* virulence and thereby found that activity and function of effector genes are specifically dependent on the host line. For future studies, it will be seminal to investigate the intraspecific variability of the maize line-specific effector genes in *U. maydis*: Are variants from different wild-type strains (Depotter *et al.*, 2021) of the same effectors functional in different host genotypes? And how does a highly specific, biotrophic pathogen like *U. maydis* co-adapt with its host maize in different ecologic backgrounds?

EXPERIMENTAL PROCEDURES

Plant growth conditions, fungal infections and collection of samples

Zea mays L. Early Golden Bantam (EGB) (Olds Seeds, Madison, WI, USA) and the inbred founder lines of the Nested Association Mapping (NAM) population (McMullen *et al.*, 2009; Yu *et al.*, 2008; North Central Regional Plant Introduction Station, IA, USA) were used for infections.

Virulence assays of *U. maydis* on *Z. mays* were performed as described in Redkar and Doehlemann (2016) in three independent biological replicates. Virulence symptoms were scored 12 dpi using the disease rating scheme developed previously (Kämper *et al.*, 2006). Disease indices were calculated as follows: The numbers of plants sorted into categories 'small tumours', 'normal tumours', 'heavy tumours' and 'dead plants' were multiplied by the number of the category (1, 3, 5 and 7, respectively), summed and then divided by the total number of infected plants: {[(1 × number of plants in category 1) + (3 × number of plants in category 3) + (5 × number of plants in category 5) + (7 × number of plants in category 7)] / total number of plants}. The resulting value for SG200 was set to unity. Indices of deletion mutants are given relative to the score for SG200. An unpaired *t*-test was used to calculate the statistical significance of the differences in disease indices between mutant strains and SG200.

Samples of 20 infected maize seedlings were collected at 1, 3, 6 and 9 dpi in three independent biological replicates. For 1 dpi, 2-cm sections of the third leaves were excised 0.5 cm below the infection holes. At later time points (3, 6 and 9 dpi), 5-cm sections of the third leaves were excised 1 cm below the infection holes. Comparable sections were harvested for mock-treated controls. For each sample, leaf sections of 20 different plants were pooled, immediately frozen in liquid nitrogen and stored at −80°C.

Generation of fungal strains

All *U. maydis* strains used in this study were derived from the solopathogenic strain SG200 (Kämper *et al.*, 2006). To generate *U. maydis* KO mutants, the CRISPR-Cas9 system using the non-integrative, self-replicating backbone plasmid pMS73 was employed (Schuster *et al.*, 2018; Schuster *et al.*, 2016). All target sequences for the guide RNA constructs were designed using the E-CRISP tool (www.e-crisp.org; Heigwer *et al.*, 2014) with medium stringency settings towards the 5′ end of the respective gene (Data Set S13). For integration into the *ip* locus of *U. maydis*, plasmids derived from p123 were used and linearised within the *cbx* gene before transformation into the respective *U. maydis* strains. Transformation of *U. maydis* was carried out as described previously (Schulz *et al.*, 1990). To identify strains with Cas9-induced mutations leading to gene KO, the respective loci were amplified and sequenced with gene-specific primers. The stable integration of p123-based plasmids into the *ip* locus was verified by Southern blot analysis. All complementation constructs were integrated in a single copy into the *U. maydis ip* locus.

Microscopic analyses

To visualise *U. maydis* infection progression, infected maize leaf samples were stained with WGA-AF488 and propidium iodide as described in Redkar *et al.* (2018) and analysed using a Zeiss Axio Zoom V16 using the GFP filter for WGA-AF488 and the DsRed filter for propidium iodide visualisation. Image processing was done using ImageJ.

Extraction of nucleic acids and RNA sequencing

For the isolation of genomic DNA from *U. maydis*, a phenol-based extraction method was used (Hoffman and Winston, 1987). For isolation of nucleic acids from maize leaves, pooled leaf sections of the individual maize samples were homogenised using a mortar and pestle under constant liquid nitrogen cooling. Isolation of genomic DNA from leaf powder was performed using the MasterPure™ Complete DNA and RNA Purification Kit from Epicentre (Epicentre, Chicago, IL, USA) according to manufacturer's instructions. For isolation of total RNA, TRIzol® reagent (Invitrogen, Darmstadt, Germany) was used according to the manufacturer's instructions. To approximately 400 μl of homogenised tissue, 1 ml TRIzol® reagent was added immediately. To eliminate genomic DNA contamination, the Turbo DNA-Free™ Kit from Ambion (Ambion Life Technologies™, Carlsbad, USA) was used according to the manufacturer's instructions. Sequencing library preparation was done using the Illumina TruSeq mRNA stranded Kit (Illumina, San Diego, CA, USA) or NEB Next® Ultra™ RNA Library Prep Kit (NEB, Ipswich, MA, USA). Illumina sequencing of mRNA was performed with 150-bp paired-end reads at the Cologne Center for Genomics (Cologne, Germany) on an Illumina HiSeq 4000 (Illumina) and at Novogene (Peking, China) on an Illumina NovaSeq 6000 (Illumina).

RNA-Seq data analysis

By Illumina sequencing of mRNA libraries, approximately 60 million 150-bp paired-end reads per *U. maydis*-infected sample and 40 million paired-end reads per mock-treated sample were created. The reads were filtered using the Trinity software (v2.9.1) option trimmomatic with standard settings (Grabherr *et al.*, 2011). The reads were then mapped to the reference genome using Bowtie 2 (v2.3.5.1) with the first 15 nucleotides on the 5′-end of the reads being trimmed (Langmead and Salzberg, 2012). As reference genome the *U. maydis* genome assembly (Kämper *et al.*, 2006) and the *Z. mays* B73 version 3 (Schnable *et al.*, 2009) genome assembly were used simultaneously. Reads were counted for *U. maydis* and *Z. mays* loci using the R (www.r-project.org) package Rsubread (v1.34.7) (Liao *et al.*, 2019). On average, 640 000 mapping read counts for the *U. maydis* genome were found per sample in the data set of different maize lines (1.3% of total read counts) and 783 000 read counts for the data set of CML322 infected by SG200 or KO_UMAG_02297 (1.8% of total read counts). For maize, approximately 50 million reads were counted for the *U. maydis*-infected samples and 43 million for the mock samples. Pre-filtering was applied to keep only genes with at least 10 counts in three samples (6284 genes for *U. maydis*, 40 056 genes for the data set of different maize lines and 30 637 genes for the data set of CML322 infected by SG200 or KO_UMAG_02297). Counts for *U. maydis* or maize were normalised and differential gene expression was analysed by DESeq2 v1.26.0

(differential expression analysis for sequence count data 2, Love *et al.*, 2014) in R. For *U. maydis*, the design formula was ~genotype, and for maize, the design formula was ~genotype+condition+genotype:condition to identify differences in condition effects (SG200-infected versus mock) between genotypes. Genes with $\log_2$(expression fold change) > 0.5 and Benjamini–Hochberg-adjusted *P* value < 0.05 were considered differentially expressed. To identify co-expressed genes, a WGCNA was performed using the WGCNA package (v1.69) (Langfelder and Horvath, 2008; Zhang and Horvath, 2005) in R. Only genes with at least 10 counts in 50% of the analysed maize samples or in 90% of the analysed *U. maydis* samples were considered. For *U. maydis*, 4013 genes and for maize 29 729 genes passed this filtering. Log_2-transformed DESeq2-normalised counts were used as input for the network analysis. The function blockwise Modules was used to create a signed network of a Pearson-correlated matrix; only positive correlations were considered. For *U. maydis,* all genes were treated in a single block. For maize, the maximum blocksize was set to 15 000. The soft power threshold was set to 4 for *U. maydis* and for maize because this was the lowest power needed to reach scale-free topology (R^2 = 0.901 and 0.871, respectively). Modules were detected using default settings with a mergeCutHeight of 0.15 and a minimal module size of 25 genes. For each module, the expression profile of the module eigengene was calculated, which represents the modules by summary expression profiles of all genes of a given module. For each gene and module eigengene, the Pearson correlation to the disease index of the different maize lines was calculated (= gene significance for the trait).

GO enrichment analysis

Gene ontology term enrichment analysis (Ashburner *et al.*, 2000; The Gene Ontology Consortium, 2017) for *U. maydis* was performed with the Gene Ontology Panther Classification System (Mi *et al.*, 2019) using a *P* value cut-off of <0.05. For the enrichment analysis of the modules correlated to the disease index, only genes were considered that had a gene significance for disease index of >0.5 or <−0.5 and a *P* value of <0.05. For maize, GO terms were annotated to the version 3 protein annotation of maize line B73 using InterProScan (v5.42-78.0) (El-Gebali *et al.*, 2019; Jones *et al.*, 2014; Schnable *et al.*, 2009). Significance of GO term enrichments in a subset of genes was calculated for all expressed genes with a Fisher exact test with the alternative hypothesis being one-sided (greater).

Quantitative reverse-transcriptase PCR and quantitative PCR

The qRT-PCRs/qPCR reactions were set up using the GoTaq® qPCR Mastermix (Promega, Madison, WI, USA) according to the manufacturer's instructions in a total volume of 15 μl. All qRT-PCRs/qPCRs were performed in an iCycler system (Bio-Rad, Munich, Germany) with the following program: 95°C for 2 min, followed by 45 cycles of 95°C for 30 s, 62°C for 30 s and 72°C for 30 s. For gene expression analysis by qRT-PCR, cDNA was synthesised from 1–5 μg of template RNA using he Thermo Scientific RevertAid H Minus First Strand cDNA Synthesis Kit (Thermo Fisher Scientific, Waltham, MA, USA) according to the manufacturer's instructions. The *U. maydis ppi* gene was used for normalisation and relative expression values were calculated using the $2^{-\Delta\Delta Ct}$ method. For fungal biomass quantification, DNA extracted from infected maize leaves was subjected to qPCR analysis with maize-specific GAPDH and *U. maydis*-specific *ppi* primers. The relative fungal biomass was calculated as the ratio of *U. maydis* DNA to maize DNA ($2^{-\Delta\Delta Ct}$).

Mapping of maize genes to Arabidopsis

For comparison to genes previously described to be involved in PTI or ETI in Arabidopsis, mapping of maize gene IDs to Arabidopsis was performed on the Monocots PLAZA 4.0 workbench (https://bioinformatics.psb.ugent.be/plaza/, Van Bel *et al.*, 2018) using the PLAZA orthologous genes integrative method with standard settings and a minimum number of required evidence types of three.

ACKNOWLEDGEMENTS

We are grateful to Benjamin Stich for generously supplying Ky21 and Tx303 seeds, to Elaine Jaeger for helping with the initial acquirement of NAM founder lines and to Mariana Schuster for providing *U. maydis* strains. We thank Henriette Läßle for excellent help with the project. Selma Schurack received support by the International Max Planck Research School of the MPIPZ, Cologne, Germany. We acknowledge the Cologne Center for Genomics (Cologne, Germany) for sequencing support. This work was funded by the European Research Council under the European Union's Horizon 2020 research and innovation programme (consolidator grant conVIRgens, ID 771035), as well as funding by the Deutsche Forschungsgemeinschaft (German Research Foundation [DFG]) under Germany's Excellence Strategy (EXC-2048/1 – Project ID: 390686111). Jasper Depotter is supported by the Research Fellowship Programme for Postdoctoral Researchers of the Alexander von Humboldt Foundation. Marco Thines and Deepak K. Gupta are supported by the LOEWE initiative of the government of Hesse, in the framework of the centre for Translational Biodiversity Genomics (TBG). Open Access funding enabled and organized by Projekt DEAL.

AUTHOR CONTRIBUTIONS

SS and GD designed the research, SS performed molecular experiments and virulence assays, SS, JD, DG and MT analysed the transcriptome data and SS and GD wrote the paper with input from all authors.

CONFLICT OF INTEREST

The authors declare no conflict of interest.

DATA AVAILABILITY STATEMENT

RNA-Seq data have been submitted to NCBI GenBank and are available under the following accession: BioProject ID: PRJNA673988.

SUPPORTING INFORMATION

Additional Supporting Information may be found in the online version of this article.

Figure S1. WGA-AF488/propidium iodide co-stained maize leaves infected with *U. maydis*.

Figure S2. Identification of genes previously associated with PTI or ETI within maize DEGs.

Figure S3. Expression of UMAG_02297 during disease progression in different maize lines.

Figure S4. Virulence functions of candidate maize line-specific effectors.

Figure S5. Virulence function of UMAG_11416 in different maize lines.

Data Set S1. DESeq2 results of *U. maydis* DEGs for all possible comparisons.

Data Set S2. Log_2-transformed relative expression levels (compared to the mean expression of all samples) of *U. maydis* differentially expressed CSEPs.

Data Set S3. WGCNA results for *U. maydis* genes.

Data Set S4. Enriched GO biological process terms in the 'greenyellow' module.

Data Set S5. Enriched GO biological process terms in the 'purple' module.

Data Set S6. DESeq2 results of maize DEGs in response to *U. maydis* for all possible comparisons.

Data Set S7. Correlation of maize gene expression to disease index.

Data Set S8. Enriched GO biological process terms in maize DEGs.

Data Set S9. Enriched GO biological process terms in maize genes positively correlated to the disease index.

Data Set S10. Enriched GO biological process terms in maize genes negatively correlated the to disease index.

Data Set S11. DEGs in the maize line CML322 between SG200 or KO infection versus mock inoculation.

Data Set S12. Enriched Interpro terms in genes uniquely regulated by SG200 or KO versus mock.

Data Set S13. Target sequences of single guide RNAs for CRISPR/Cas9 KO and induced mutations.

REFERENCES

Ashburner, M., Ball, C.A., Blake, J.A., Botstein, D., Butler, H., Cherry, J.M. *et al.* (2000) Gene ontology: Tool for the unification of biology. *Nature Genetics*, **25**, 25–29. https://doi.org/10.1038/75556

Bacete, L., Mélida, H., López, G., Dabos, P., Tremousaygue, D., Denancé, N. *et al.* (2020) Arabidopsis response regulator 6 (ARR6) modulates plant cell-wall composition and disease resistance. *Molecular Plant-Microbe Interactions Journal*, **33**, 767–780. https://doi.org/10.1094/MPMI-12-19-0341-R.

Bao, Z., Yang, H. & Hua, J. (2013) Perturbation of cell cycle regulation triggers plant immune response via activation of disease resistance genes. *Proceedings of the National Academy of Sciences*, **110**, 2407–2412. https://doi.org/10.1073/pnas.1217024110.

Barbacci, A., Navaud, O., Mbengue, M., Barascud, M., Godiard, L., Khafif, M. *et al.* (2020) Rapid identification of an Arabidopsis NLR gene as a candidate conferring susceptibility to *Sclerotinia sclerotiorum* using time-resolved automated phenotyping. *The Plant Journal*, **103**, 903–917. https://doi.org/10.1111/tpj.14747.

Bartoli, C. & Roux, F. (2017) Genome-wide association studies in plant pathosystems: toward an ecological genomics approach. *Frontiers in Plant Science*, https://doi.org/10.3389/fpls.2017.00763.

Basse, C.W. & Steinberg, G. (2004) *Ustilago maydis*, model system for analysis of the molecular basis of fungal pathogenicity. *Molecular Plant Pathology*, **5**, 83–92. https://doi.org/10.1111/j.1364-3703.2004.00210.x.

Baumgarten, A.M., Suresh, J., May, G. & Phillips, R.L. (2007) Mapping QTLs contributing to *Ustilago maydis* resistance in specific plant tissues of maize. *Theoretical and Applied Genetics*, **114**, 1229–1238. https://doi.org/10.1007/s00122-007-0513-5.

Bölker, M., Urban, M. & Kahmann, R. (1992) The a mating type locus of *U. maydis* specifies cell signaling components. *Cell*, **68**, 441–450. https://doi.org/10.1016/0092-8674(92)90182-C.

Brefort, T., Doehlemann, G., Mendoza-Mendoza, A., Reissmann, S., Djamei, A., Kallmann, R. *et al.* (2009) *Ustilago maydis* as a pathogen. *Annual Review of Phytopathology*, **47**, 423–445. https://doi.org/10.1146/annurev-phyto-080508-081923.

Cook, D.E., Lee, T.G., Guo, X., Melito, S., Wang, K., Bayless, A.M. *et al.* (2012) Copy number variation of multiple genes at Rhg1 mediates nematode resistance in soybean. *Science*, **338**(6111), 1206–1209. https://doi.org/10.1126/science.1228746.

Corwin, J.A. & Kliebenstein, D.J. (2017) Quantitative resistance: more than just perception of a pathogen. *The Plant Cell*, **29**, 655–665. https://doi.org/10.1105/tpc.16.00915.

Cui, F., Wu, S., Sun, W., Coaker, G., Kunkel, B., He, P. *et al.* (2013) The *Pseudomonas syringae* type III effector AvrRpt2 promotes pathogen virulence via stimulating Arabidopsis auxin/indole acetic acid protein turnover. *Plant Physiology*, https://doi.org/10.1104/pp.113.219659.

Cui, H., Tsuda, K. & Parker, J.E. (2015) Effector-triggered immunity: from pathogen perception to robust defense. *Annual Review of Plant Biology*, **66**, 487–511. https://doi.org/10.1146/annurev-arplant-050213-040012.

Dangl, J.L. & Jones, J.D.G. (2001) Plant pathogens and integrated defence responses to infection. *Nature*, **411**, 826–833. https://doi.org/10.1038/35081161.

Dean, R., Van Kan, J.A.L., Pretorius, Z.A., Hammond-Kosack, K.E., Di Pietro, A., Spanu, P.D. *et al.* (2012) The top 10 fungal pathogens in molecular plant pathology. *Molecular Plant Pathology*, **13**, 414–430. https://doi.org/10.1111/j.1364-3703.2011.00783.x.

Delplace, F., Huard-Chauveau, C., Dubiella, U., Khafif, M., Alvarez, E., Langin, G. *et al.* (2020) Robustness of plant quantitative disease resistance is provided by a decentralized immune network. *Proceedings of the National Academy of Sciences*, **117**, 18099–18109. https://doi.org/10.1073/pnas.2000078117.

Depotter, J.R.L., Zuo, W., Hansen, M., Zhang, B., Xu, M. & Doehlemann, G. (2021) Effectors with different gears: divergence of *Ustilago maydis* effector genes is associated with their temporal expression pattern during plant infection. *Journal of Fungi*, **7**, 1–14. https://doi.org/10.3390/jof7010016.

Djamei, A., Schipper, K., Rabe, F., Ghosh, A., Vincon, V., Kahnt, J. *et al.* (2011) Metabolic priming by a secreted fungal effector. *Nature*, **478**, 395–398. https://doi.org/10.1038/nature10454.

Doehlemann, G., van der Linde, K., Aßmann, D., Schwammbach, D., Hof, A., Mohanty, A. *et al.* (2009) Pep1, a secreted effector protein of *Ustilago maydis*, is required for successful invasion of plant cells. *PLoS Path*, **5**, e1000290. https://doi.org/10.1371/journal.ppat.1000290.

Doehlemann, G., Wahl, R., Horst, R.J., Voll, L.M., Usadel, B., Poree, F. *et al.* (2008a) Reprogramming a maize plant: transcriptional and metabolic changes induced by the fungal biotroph *Ustilago maydis*. *The Plant Journal*, **56**, 181–195. https://doi.org/10.1111/j.1365-313X.2008.03590.x.

Doehlemann, G., Wahl, R., Vranes, M., de Vries, R.P., Kämper, J. & Kahmann, R. (2008b) Establishment of compatibility in the *Ustilago maydis*/maize pathosystem. *Journal of Plant Physiology*, **165**, 29–40. https://doi.org/10.1016/j.jplph.2007.05.016.

Dong, S., Stam, R., Cano, L.M., Song, J., Sklenar, J., Yoshida, K. *et al.* (2014) Effector specialization in a lineage of the Irish potato famine pathogen. *Science*, **343**(6170), 552–555. https://doi.org/10.1126/science.1246300.

Dong, X., Jiang, Z., Peng, Y.L. & Zhang, Z. (2015) Revealing shared and distinct gene network organization in Arabidopsis immune responses by integrative analysis. *Plant Physiology*, **167**(3), 1186–1203. https://doi.org/10.1104/pp.114.254292.

Dutheil, J.Y., Mannhaupt, G., Schweizer, G., Sieber, C.M.K., Münsterkötter, M., Güldener, U. *et al.* (2016) A tale of genome compartmentalization: the evolution of virulence clusters in smut fungi. *Genome Biology and Evolution*, **8**, 681–704. https://doi.org/10.1093/gbe/evw026.

El-Gebali, S., Mistry, J., Bateman, A., Eddy, S.R., Luciani, A., Potter, S.C. *et al.* (2019) The Pfam protein families database in 2019. *Nucleic Acids Research*, **47**, D427–D432. https://doi.org/10.1093/nar/gky995.

Evangelisti, E., Govetto, B., Minet-Kebdani, N., Kuhn, M.-L., Attard, A., Ponchet, M. *et al.* (2013) The *Phytophthora parasitica* RXLR effector penetration-specific effector 1 favours *Arabidopsis thaliana* infection by interfering with auxin physiology. *New Phytologist*, **199**, 476–489. https://doi.org/10.1111/nph.12270.

Fukuoka, S., Saka, N., Koga, H., Ono, K., Shimizu, T., Ebana, K. *et al.* (2009) Loss of function of a proline-containing protein confers durable disease resistance in rice. *Science*, **325**(5943), 998–1001. https://doi.org/10.1126/science.1175550.

Gianinazzi-Pearson, V., Smith, S.E., Gianinazzi, S. & Smith, F.A. (1991) Enzymatic studies on the metabolism of vesicular-arbuscular mycorrhizas. V. Is H+-ATPase a component of ATP-hydrolysing enzyme activities in plant-fungus interfaces? *New Phytologist*, **117**, 61–74. https://doi.org/10.1111/j.1469-8137.1991.tb00945.x.

Grabherr, M.G., Haas, B.J., Yassour, M., Levin, J.Z., Thompson, D.A., Amit, I. *et al.* (2011) Full-length transcriptome assembly from RNA-Seq data without a reference genome. *Nature Biotechnology*, **29**, 644–652. https://doi.org/10.1038/nbt.1883.

Hatsugai, N., Igarashi, D., Mase, K., Lu, Y., Tsuda, Y., Chakravarthy, S. *et al.* (2017) A plant effector-triggered immunity signaling sector is inhibited by pattern-triggered immunity. *EMBO Journal*, **36**, 2758–2769. https://doi.org/10.15252/embj.201796529.

Hazen, S.P., Hawley, R.M., Davis, G.L., Henrissat, B. & Walton, J.D. (2003) Quantitative trait loci and comparative genomics of cereal cell wall composition. *Plant Physiology*, **132**, 263–271. https://doi.org/10.1104/pp.103.020016.

Heigwer, F., Kerr, G. & Boutros, M. (2014) E-CRISP: fast CRISPR target site IDENTIFICATION. *Nature Methods*, **11**, 122–123. https://doi.org/10.1038/nmeth.2812.

Hoffman, C.S. & Winston, F. (1987) A ten-minute DNA preparation from yeast efficiently releases autonomous plasmids for transformation of *Escherichia coli*. *Gene*, **57**, 267–272. https://doi.org/10.1016/0378-1119(87)90131-4.

Hoover, M.M. (1932) Inheritance studies of the reaction to selfed lines of maize to smut (*Ustilago zeae*). West VirginiaAgricultural and Forestry Experiment Station Bulletins. 253.

Horst, R.J., Doehlemann, G., Wahl, R., Hofmann, J., Schmiedl, A., Kahmann, R. *et al.* (2010) A model of *Ustilago maydis* leaf tumor metabolism. *Plant Signal Behaviour*, **5**, 1446–1449. https://doi.org/10.4161/psb.5.11.13360.

Horst, R.J., Engelsdorf, T., Sonnewald, U. & Voll, L.M. (2008) Infection of maize leaves with *Ustilago maydis* prevents establishment of C4 photosynthesis. *Journal of Plant Physiology*, **165**(1), 19–28. https://doi.org/10.1016/j.jplph.2007.05.008.

Hurni, S., Scheuermann, D., Krattinger, S.G., Kessel, B., Wicker, T., Herren, G. *et al.* (2015) The maize disease resistance gene Htn1 against northern corn leaf blight encodes a wall-associated receptor-like kinase. *Proceedings of the National Academy of Sciences*, **112**, 8780–8785. https://doi.org/10.1073/pnas.1502522112.

Immer, F.R. (1927) The inheritance of reaction to *Ustilago zeae* in maize. Minn. Agric. Exp. Sta. Techn. Bull. 51

Jones, P., Binns, D., Chang, H.Y., Fraser, M., Li, W., McAnulla, C. *et al.* (2014) InterProScan 5: genome-scale protein function classification. *Bioinformatics*, **30**, 1236–1240. https://doi.org/10.1093/bioinformatics/btu031.

Jubault, M., Lariagon, C., Taconnat, L., Renou, J.-P., Gravot, A., Delourme, R. *et al.* (2013) Partial resistance to clubroot in Arabidopsis is based on changes in the host primary metabolism and targeted cell division and expansion capacity. *Functional & Integrative Genomics*, **13**, 191–205. https://doi.org/10.1007/s10142-013-0312-9.

Kämper, J. (2004) A PCR-based system for highly efficient generation of gene replacement mutants in *Ustilago maydis*. *Molecular Genetics and Genomics*, **271**, 103–110. https://doi.org/10.1007/s00438-003-0962-8.

Kämper, J., Kahmann, R., Bölker, M., Ma, L.-J., Brefort, T., Saville, B.J. *et al.* (2006) Insights from the genome of the biotrophic fungal plant pathogen *Ustilago maydis*. *Nature*, **444**, 97–101. https://doi.org/10.1038/nature05248.

Kazan, K. & Manners, J.M. (2009) Linking development to defense: auxin in plant–pathogen interactions. *Trends in Plant Science*, **14**, 373–382. https://doi.org/10.1016/j.tplants.2009.04.005.

Kebede, A.Z., Johnston, A., Schneiderman, D., Bosnich, W. & Harris, L.J. (2018) Transcriptome profiling of two maize inbreds with distinct responses to Gibberella ear rot disease to identify candidate resistance genes. *BMC Genomics*, **19**, 131. https://doi.org/10.1186/s12864-018-4513-4.

Krattinger, S.G., Lagudah, E.S., Spielmeyer, W., Singh, R.P., Huerta-Espino, J., McFadden, H. *et al.* (2009) A putative ABC transporter confers durable resistance to multiple fungal pathogens in wheat. *Science*, **323**(5919), 1360–1363. https://doi.org/10.1126/science.1166453.

Kretschmer, M., Croll, D. & Kronstad, J.W. (2017) Maize susceptibility to *Ustilago maydis* is influenced by genetic and chemical perturbation of carbohydrate allocation. *Molecular Plant Pathology*, **18**, 1222–1237. https://doi.org/10.1111/mpp.12486.

Langfelder, P. & Horvath, S. (2008) WGCNA: an R package for weighted correlation network analysis. *BMC Bioinformatics*, **9**, 559. https://doi.org/10.1186/1471-2105-9-559.

Langmead, B. & Salzberg, S.L. (2012) Fast gapped-read alignment with Bowtie 2. *Nature Methods*, **9**, 357–359. https://doi.org/10.1038/nmeth.1923.

Lanver, D., Müller, A.N., Happel, P., Schweizer, G., Haas, F.B., Franitza, M. *et al.* (2018) The biotrophic development of *Ustilago maydis* studied by RNA-Seq analysis. *The Plant Cell*, **30**, 300–323. https://doi.org/10.1105/tpc.17.00764.

Liao, Y., Smyth, G.K. & Shi, W. (2019) The R package Rsubread is easier, faster, cheaper and better for alignment and quantification of RNA sequencing reads. *Nucleic Acids Research*, **47**, e47. https://doi.org/10.1093/nar/gkz114.

Love, M.I., Huber, W. & Anders, S. (2014) Moderated estimation of fold change and dispersion for RNA-seq data with DESeq2. *Genome Biology*, **15**, 1–21. https://doi.org/10.1186/s13059-014-0550-8.

Lübberstedt, T., Klein, D. & Melchinger, A.E. (1998) Comparative QTL mapping of resistance to *Ustilago maydis* across four populations of European flint-maize. *Theoretical and Applied Genetics*, **97**, 1321–1330. https://doi.org/10.1007/s001220051025.

Ma, L.-S., Wang, L., Trippel, C., Mendoza-Mendoza, A., Ullmann, S., Moretti, M. *et al.* (2018) The *Ustilago maydis* repetitive effector Rsp3 blocks the antifungal activity of mannose-binding maize proteins. *Nature Communications*, **9**, 1711. https://doi.org/10.1038/s41467-018-04149-0.

Matei, A., Ernst, C., Günl, M., Thiele, B., Altmüller, J., Walbot, V. *et al.* (2018) How to make a tumour: cell type specific dissection of *Ustilago maydis*-induced tumour development in maize leaves. *New Phytologist*, **217**, 1681–1695. https://doi.org/10.1111/nph.14960.

McHale, L., Tan, X., Koehl, P. & Michelmore, R.W. (2006) Plant NBS-LRR proteins: adaptable guards. *Genome Biology*, **7**, 212. https://doi.org/10.1186/gb-2006-7-4-212.

McMullen, M.D., Kresovich, S., Villeda, H.S., Bradbury, P., Li, H., Sun, Q. *et al.* (2009) Genetic properties of the maize nested association mapping population. *Science*, **325**, 737–740. https://doi.org/10.1126/science.1174320.

Meihls, L.N., Handrick, V., Glauser, G., Barbier, H., Kaur, H., Haribal, M.M. *et al.* (2013) Natural variation in maize aphid resistance is associated with 2,4-dihydroxy-7-methoxy-1,4-benzoxazin-3-one glucoside methyltransferase activity. *The Plant Cell*, **25**, 1–16. https://doi.org/10.1105/tpc.113.112409.

Mi, H., Muruganujan, A., Ebert, D., Huang, X. & Thomas, P.D. (2019) PANTHER version 14: more genomes, a new PANTHER GO-slim and improvements in enrichment analysis tools. *Nucleic Acids Research*, **47**, D419–D426. https://doi.org/10.1093/nar/gky1038.

Mine, A., Seyfferth, C., Kracher, B., Berens, M.L., Becker, D. & Tsuda, K. (2018) The defense phytohormone signaling network enables rapid, high-amplitude transcriptional reprogramming during effector-triggered immunity. *The Plant Cell*, **30**, 1199–1219. https://doi.org/10.1105/tpc.17.00970.

Mueller, A.N., Ziemann, S., Treitschke, S., Aßmann, D. & Doehlemann, G. (2013) Compatibility in the *Ustilago maydis*–maize interaction requires inhibition of host cysteine proteases by the fungal effector Pit2. *PLoS Path*, **9**, e1003177. https://doi.org/10.1371/journal.ppat.1003177.

Müller, O., Schreier, P.H. & Uhrig, J.F. (2008) Identification and characterization of secreted and pathogenesis-related proteins in *Ustilago maydis*. *Molecular Genetics and Genomics*, **279**, 27–39. https://doi.org/10.1007/s00438-007-0291-4.

Mutka, A.M., Fawley, S., Tsao, T. & Kunkel, B.N. (2013) Auxin promotes susceptibility to *Pseudomonas syringae* via a mechanism independent of suppression of salicylic acid-mediated defenses. *The Plant Journal*, **74**, 746–754. https://doi.org/10.1111/tpj.12157.

Navarro, L., Dunoyer, P., Jay, F., Arnold, B., Dharmasiri, N., Estelle, M. *et al.* (2006) A plant miRNA contributes to antibacterial resistance by repressing auxin signaling. *Science*, **312**(5772), 436–439. https://doi.org/10.1126/science.1126088.

Niks, R.E., Qi, X. & Marcel, T.C. (2015) Quantitative resistance to biotrophic filamentous plant pathogens: concepts, misconceptions, and mechanisms. *Annual review of Phytopathology*, **53**, 445–470. https://doi.org/10.1146/annurev-phyto-080614-115928.

Ökmen, B., Kemmerich, B., Hilbig, D., Wemhöner, R., Aschenbroich, J., Perrar, A. *et al.* (2018) Dual function of a secreted fungalysin metalloprotease in *Ustilago maydis*. *New Phytologist*, **220**, 249–261. https://doi.org/10.1111/nph.15265.

Ospina-Giraldo, M.D., Mullins, E. & Kang, S. (2003) Loss of function of the *Fusarium oxysporum* SNF1 gene reduces virulence on cabbage and Arabidopsis. *Current Genetics*, **44**, 49–57. https://doi.org/10.1007/s00294-003-0419-y.

Palmgren, M.G. (1990) An H + -ATPase assay: proton pumping and ATPase activity determined simultaneously in the same sample. *Plant Physiology*, **94**, 882–886. https://doi.org/10.1104/pp.94.3.882.

Pan, Y., Liu, Z., Rocheleau, H., Fauteux, F., Wang, Y., McCartney, C. *et al.* (2018) Transcriptome dynamics associated with resistance and susceptibility against Fusarium head blight in four wheat genotypes. *BMC Genomics*, **19**, 642. https://doi.org/10.1186/s12864-018-5012-3.

Poland, J.A., Balint-Kurti, P.J., Wisser, R.J., Pratt, R.C. & Nelson, R.J. (2009) Shades of gray: the world of quantitative disease resistance. *Trends in Plant Science*, **14**, 21–29. https://doi.org/10.1016/j.tplants.2008.10.006.

Poland, J.A., Bradbury, P.J., Buckler, E.S. & Nelson, R.J. (2011) Genome-wide nested association mapping of quantitative resistance to northern leaf blight in maize. *Proceedings of the National Academy of Sciences*, **108**, 6893–6898. https://doi.org/10.1073/pnas.1010894108.

Redkar, A. & Doehlemann, G. (2016) *Ustilago maydis* virulence assays in maize. *Bio-protocol*, **6**, e1760. https://doi.org/10.21769/BioProtoc.1760.

Redkar, A., Hoser, R., Schilling, L., Zechmann, B., Krzymowska, M., Walbot, V. *et al.* (2015) A secreted effector protein of *Ustilago maydis* guides maize leaf cells to form tumors. *The Plant Cell*, **27**, 1332–1351. https://doi.org/10.1105/tpc.114.131086.

Redkar, A., Jaeger, E. & Doehlemann, G. (2018) Visualization of growth and morphology of fungal hyphae in planta using WGA-AF488 and propidium iodide co-staining. *Bio-protocol*, **8**, e2942. https://doi.org/10.21769/BioProtoc.2942.

Reineke, G., Heinze, B., Schirawski, J., Buettner, H., Kahmann, R. & Basse, C.W. (2008) Indole-3-acetic acid (IAA) biosynthesis in the smut fungus *Ustilago maydis* and its relevance for increased IAA levels in infected tissue and host tumour formation. *Mol Plant Pathol*, https://doi.org/10.1111/j.1364-3703.2008.00470.x.

Robles-Martínez, L., Pardo, J.P., Miranda, M., Mendez, T.L., Matus-Ortega, M.G., Mendoza-Hernández, G. *et al.* (2013) The basidiomycete *Ustilago maydis* has two plasma membrane H +-ATPases related to fungi and plants. *Journal of Bioenergetics and Biomembranes*, **45**, 477–490. https://doi.org/10.1007/s10863-013-9520-1.

Roux, F., Voisin, D., Badet, T., Balagué, C., Barlet, X., Huard-Chauveau, C. *et al.* (2014) Resistance to phytopathogens e tutti quanti: placing plant quantitative disease resistance on the map. *Molecular Plant Pathology*, **15**, 427–432. https://doi.org/10.1111/mpp.12138.

Schilling, L., Matei, A., Redkar, A., Walbot, V. & Doehlemann, G. (2014) Virulence of the maize smut *Ustilago maydis* is shaped by organ-specific effectors. *Molecular Plant Pathology*, **15**, 780–789. https://doi.org/10.1111/mpp.12133.

Schirawski, J., Mannhaupt, G., Münch, K., Brefort, T., Schipper, K., Doehlemann, G. *et al.* (2010) Pathogenicity determinants in smut fungi revealed by genome comparison. *Science*, **330**(6010), 1546–1548. https://doi.org/10.1126/science.1195330.

Schnable, P.S., Ware, D., Fulton, R.S., Stein, J.C., Wei, F., Pasternak, S. *et al.* (2009) The B73 maize genome: complexity, diversity, and dynamics. *Science*, **326**(5956), 1112–1115.

Schuler, D., Wahl, R., Wippel, K., Vranes, M., Münsterkötter, M., Sauer, N. *et al.* (2015) Hxt1, a monosaccharide transporter and sensor required for virulence of the maize pathogen *Ustilago maydis*. *New Phytologist*, **206**, 1086–1100. https://doi.org/10.1111/nph.13314.

Schulz, B., Banuett, F., Dahl, M., Schlesinger, R., Schäfer, W., Martin, T. *et al.* (1990) The b alleles of *U. maydis*, whose combinations program pathogenic development, code for polypeptides containing a homeodomain-related motif. *Cell*, **60**, 295–306. https://doi.org/10.1016/0092-8674(90)90744-Y.

Schuster, M., Schweizer, G. & Kahmann, R. (2018) Comparative analyses of secreted proteins in plant pathogenic smut fungi and related basidiomycetes. *Fungal Genetics and Biology*, **112**, 21–30. https://doi.org/10.1016/j.fgb.2016.12.003.

Schuster, M., Schweizer, G., Reissmann, S. & Kahmann, R. (2016) Genome editing in *Ustilago maydis* using the CRISPR-Cas system. *Fungal Genetics and Biology*, **89**, 3–9. https://doi.org/10.1016/j.fgb.2015.09.001.

Skibbe, D.S., Doehlemann, G., Fernandes, J. & Walbot, V. (2010) Maize tumors caused by *Ustilago maydis* require organ-specific genes in host and pathogen. *Science*, **328**(5974), 89–92. https://doi.org/10.1126/science.1185775.

Sharma, R., Ökmen, B., Doehlemann, G. & Thines, M. (2019) Saprotrophic yeasts formerly classified as Pseudozyma have retained a large effector arsenal, including functional Pep1 orthologs. *Mycological Progress*, **18**, 763–768.

Sondergaard, T.E., Schulz, A. & Palmgren, M.G. (2004) Energization of transport processes in plants. Roles of the plasma membrane H + -ATPase. *Plant Physiology*, **136**, 2475–2482. https://doi.org/10.1104/pp.104.048231.

Spellig, T., Regenfelder, E., Reichmann, M., Schauwecker, F., Bohlmann, R., Urban, M. *et al.* (1994) Control of mating and development in *Ustilago maydis*. *Antonie van Leeuwenhoek*, **65**, 191–197. https://doi.org/10.1007/BF00871946.

St.Clair, D.A. (2010) Quantitative disease resistance and quantitative resistance loci in breeding. *Annual review of Phytopathology*, **48**, 247–268. https://doi.org/10.1146/annurev-phyto-080508-081904.

Stasko, A.K., Batnini, A., Bolanos-Carriel, C., Lin, J.E., Lin, Y., Blakeslee, J.J. & *et al.* (2020) Auxin profiling and GmPIN expression in *Phytophthora sojae* –soybean root interactions. *Phytopathology*® PHYTO-02-20-004. https://doi.org/10.1094/PHYTO-02-20-0046-R.

Stirnberg, A. & Djamei, A. (2016) Characterization of ApB73, a virulence factor important for colonization of *Zea mays* by the smut *Ustilago maydis*. *Molecular Plant Pathology*, **17**, 1467–1479. https://doi.org/10.1111/mpp.12442.

Tanaka, S., Brefort, T., Neidig, N., Djamei, A., Kahnt, J., Vermerris, W. *et al.* (2014) A secreted *Ustilago maydis* effector promotes virulence by targeting anthocyanin biosynthesis in maize. *Elife*, **3**, e01355. https://doi.org/10.7554/eLife.01355.001.

The Gene Ontology Consortium (2017) Expansion of the gene ontology knowledgebase and resources. *Nucleic Acids Research*, **45**, D331–D338. https://doi.org/10.1093/nar/gkw1108.

Tonukari, N.J., Scott-Craig, J.S. & Waltonb, J.D. (2000) The *Cochliobolus carbonum* SNF1 gene is required for cell wall-degrading enzyme expression and virulence on maize. *The Plant Cell*, **12**, 237–247. https://doi.org/10.1105/tpc.12.2.237.

Turian, G. & Hamilton, R.H. (1960) Chemical detection of 3-indolylacetic acid in *Ustilago zeae* tumors. *Biochimica et Biophysica Acta*, **41**, 148–150. https://doi.org/10.1016/0006-3002(60)90381-4.

Van Bel, M., Diels, T., Vancaester, E., Kreft, L., Botzki, A., Van de Peer, Y. *et al.* (2018) PLAZA 4.0: an integrative resource for functional, evolutionary and comparative plant genomics. *Nucleic Acids Research*, **46**, D1190–D1196. https://doi.org/10.1093/nar/gkx1002.

Villajuana-Bonequi, M., Matei, A., Ernst, C., Hallab, A., Usadel, B. & Doehlemann, G. (2019) Cell type specific transcriptional reprogramming of maize leaves during *Ustilago maydis* induced tumor formation. *Scientific Reports*, **9**, 1–15. https://doi.org/10.1038/s41598-019-46734-3.

Vogel, J.P., Raab, T.K., Schiff, C. & Somerville, S.C. (2002) PMR6, a pectate lyase-like gene required for powdery mildew susceptibility in Arabidopsis. *The Plant Cell*, **14**, 2095–2106. https://doi.org/10.1105/tpc.003509.

Vorwerk, S., Somerville, S. & Somerville, C. (2004) The role of plant cell wall polysaccharide composition in disease resistance. *Trends in Plant Science*, **9**, 203–209. https://doi.org/10.1016/j.tplants.2004.02.005.

Wahl, R., Wippel, K., Goos, S., Kämper, J. & Sauer, N. (2010) A novel high-affinity sucrose transporter is required for virulence of the plant pathogen *Ustilago maydis*. *PLoS Biology*, **8**, e1000303. https://doi.org/10.1371/journal.pbio.1000303.

Wang, D., Pajerowska-Mukhtar, K., Culler, A.H. & Dong, X. (2007) Salicylic acid inhibits pathogen growth in plants through repression of the auxin signaling pathway. *Current Biology*, **17**, 1784–1790. https://doi.org/10.1016/j.cub.2007.09.025.

Wang, E., Yu, N., Bano, S.A., Liu, C., Miller, A.J., Cousins, D. *et al.* (2014) A H + -ATPase that energizes nutrient uptake during mycorrhizal symbioses in rice and *Medicago truncatula*. *The Plant Cell*, **26**, 1818–1830. https://doi.org/10.1105/tpc.113.120527.

Wiethölter, N., Graeßner, B., Mierau, M., Mort, A.J. & Moerschbacher, B.M. (2003) Differences in the methyl ester distribution of homogalacturonans from near-isogenic wheat lines resistant and susceptible to the wheat stem rust fungus. *Molecular Plant-Microbe Interactions*, **16**, 945–952. https://doi.org/10.1094/MPMI.2003.16.10.945.

Yang, Q., He, Y., Kabahuma, M., Chaya, T., Kelly, A., Borrego, E. *et al.* (2017) A gene encoding maize caffeoyl-CoA O-methyltransferase confers quantitative resistance to multiple pathogens. *Nature Genetics*, **49**, 1364–1372. https://doi.org/10.1038/ng.3919.

Ye, J., Zhong, T., Zhang, D., Ma, C., Wang, L., Yao, L. *et al.* (2019) The auxin-regulated protein ZmAuxRP1 coordinates the balance between

root growth and stalk rot disease resistance in maize. *Molecular Plant*, **12**, 360–373. https://doi.org/10.1016/j.molp.2018.10.005.

Yu, J., Holland, J.B., McMullen, M.D. & Buckler, E.S. (2008) Genetic design and statistical power of nested association mapping in maize. *Genetics*, **178**, 539–551. https://doi.org/10.1534/genetics.107.074245.

Zhang, B. & Horvath, S. (2005) A general framework for weighted gene co-expression network analysis. *Statistical Applications in Genetics and Molecular Biology*, https://doi.org/10.2202/1544-6115.1128.

Zuo, W., Chao, Q., Zhang, N., Ye, J., Tan, G., Li, B. *et al.* (2015) A maize wall-associated kinase confers quantitative resistance to head smut. *Nature Genetics*, **47**, 151–157. https://doi.org/10.1038/ng.3170.

Zuo, W., Depotter, J.R. & Doehlemann, G. (2020) Cas9HF1 enhanced specificity in *Ustilago maydis*. *Fungal Biology*, **124**, 228–234. https://doi.org/10.1016/j.funbio.2020.02.006.

Zuo, W., Oekmen, B., Depotter, J.R.L., Ebert, M.K., Redkar, A., Misas Villamil, J. *et al.* (2019) Molecular interactions between smut fungi and their host plants. *Annual Review of Phytopathology*, **57**, 411–430. https://doi.org/10.1146/annurev-phyto-082718-100139.